CUKUROVA UNIVERSITY
INSTITUTE OF NATURAL AND APPLIED SCIENCES

MSc THESIS

Syed Hamza Zaffar BUKHARI

LIPOSOMAL AND SILVER ENCAPSULATION OF CANCER DRUG L24 FOR DRUG DELIVERY SYSTEM AGAINST LUNGS CANCER

DEPARTMENT OF BIOTECHNOLOGY

ADANA-2023

ÇUKUROVA ÜNİVERSITY
INSTITUTE OF NATURAL AND APPLIED SCIENCES

LIPOSOMAL AND SILVER ENCAPSULATION OF CANCER DRUG L24 FOR DRUG DELIVERY SYSTEM AGAINST LUNGS CANCER

Syed Hamza Zaffar BUKHARI

MSc THESIS

DEPARTMENT OF BIOTECHNOLOGY

We certify that the thesis titled above was reviewed and approved fort he award of the degree of the Master of Science by the board of jury on 05/01/2023

……..	……..	……
Doç Dr. Yasemin SAYGIDEĞER	Prof. Dr. Bertan YILMAZ	Doç. Dr. Doğan KAYA
DANIŞMAN	ÜYE	ÜYE

MSc Thesis is written at the Department of Biotechnology of Institute of Natural and Applied Sciences of Cukurova University
Register Number:

Prof. Dr. Sadık DİNÇER
Director
Institute of Natural and Applied Science

This study was supported by the Research Fund Project of Çukurova University
Project No: FYL-2021-14367

ABSTRACT

MSc THESIS

LIPOSOMAL AND SILVER ENCAPSULATION OF CANCER DRUG L24 FOR DRUG DELIVERY SYSTEM AGAINST LUNGS CANCER

Syed Hamza Zaffar BUKHARI

ÇUKUROVA UNIVERSITY I
NSTITUTE OF NATURAL AND APPLIED SCIENCES
DEPARTMENT OF BIOTECHNOLOGY

Supervisor : Assoc. Prof. Dr. Yasemin SAYGIDEĞER
Year: 2023, Pages:69
Jury : Assoc. Prof. Dr. Yasemin SAYGIDEĞER
: Prof. Dr. Bertan YILMAZ
: Assoc. Prof. Dr. Doğan KAYA

Nowadays, there has been a significant increase in the usage of different kind of nanoparticles within the biomedical field with the rapid developments in nanotechnology. Nanoparticles are actually particles ranging in size between 1 and 100 nm. Due to their biological and physicochemical therapeutic qualities, silver nanoparticles (AgNPs) have been widely exploited in biomedicine. Silver nanoparticles also have anti-inflammatory, anti-viral, anti-angiogenic, anti-fungal, anti-bacterial and anti-cancer biological activities. Because of their unique physical, chemical, and optical properties, particularly enable them to be used in a variety of applications, including the delivery of medications to a specific target inside the body, silver nanoparticles are being studied more and more. Approaches that circumvent these challenges are crucial given the drawbacks of standard cancer treatment, which include low absorption and the resultant need for high doses that have negative side effects. This study was conducted to assess the efficacy of drug L24, silver nanoparticles and coupling of Ag-L24 on human lung cancer cell line A-549. And these three treatments were also applied to Human Normal lungs epithelial cell line Beas2B to assess the viability using MTT Assay. The results of this study present an overview of silver nanoparticles as a drug carrier system, transport of anticancer drugs, specificity and compare hemolytic toxicity between free drug and drug with silver nanoparticles. The viability assay and the calculation of IC value and cell viability assay show promising results.

Key words: Nano particles, Cancer, Liposomes, Silver nanoparticles, Drug Carrier

ÖZ

YÜKSEK LİSANS TEZİ

AKCİĞER KANSERİNE KARŞI İLAÇ VERME SİSTEMİ İÇİN KANSER İLACI L24'ün LİPOZOMAL VE GÜMÜŞ KAPSÜLLENMESİ.

Syed Hamza Zaffar BUKHARI

ÇUKUROVA ÜNİVERSİTESİ
FEN BİLİMLERİ ENSTİTÜSÜ
BİYOTEKNOLOJİ ANABİLİM DALI

Danışman : Dr. Öğr. Üyesi Yasemin SAYGIDEĞER
Yıl: 2019, Sayfa:69
Jüri : Dr. Öğr. Üyesi Yasemin SAYGIDEĞER
: Prof. Dr. Bertan YILMAZ
: Doç. Dr. Doğan KAYA

Günümüzde nanoteknolojideki hızlı gelişmelerle birlikte farklı türde nanoparçacıkların biyomedikal alanda kullanımında önemli bir artış olmuştur. Nanopartiküller aslında boyutları 1-100 nm arasında değişen parçacıklardır. Biyolojik ve fizikokimyasal terapötik nitelikleri nedeniyle, gümüş nanopartiküller (AgNP'ler) biyotıpta yaygın olarak kullanılmaktadır. Gümüş nanoparçacıklar ayrıca anti-enflamatuar, anti-viral, anti-anjiyojenik, anti-fungal, anti-bakteriyel ve anti-kanser biyolojik aktivitelerine sahiptir. Eşsiz fiziksel, kimyasal ve optik özellikleri nedeniyle, özellikle ilaçların vücuttaki belirli bir hedefe verilmesi de dahil olmak üzere çeşitli uygulamalarda kullanılmalarına olanak sağladığından, gümüş nanopartiküller üzerinde giderek daha fazla çalışılmaktadır. Standart kanser tedavisinin düşük absorpsiyon ve bunun sonucunda olumsuz yan etkileri olan yüksek dozlara duyulan ihtiyacı içeren dezavantajları göz önüne alındığında, bu zorlukların üstesinden gelen yaklaşımlar çok önemlidir. Bu çalışma, ilaç L24'ün, gümüş nanopartiküllerin ve Ag-L24'ün insan akciğer kanseri hücre dizisi A-549 üzerindeki etkinliğini değerlendirmek için yapılmıştır. Ve bu üç tedavi, MTT testi kullanılarak yaşayabilirliği değerlendirmek için İnsan Normal akciğer epitel hücre hattı Beas2B'ye de uygulandı. Bu çalışmanın sonuçları, bir ilaç taşıyıcı sistem olarak gümüş nanoparçacıklara, antikanser ilaçların taşınmasına, özgüllüğe genel bir bakış sunar ve serbest ilaç ile gümüş nanoparçacıkları olan ilaç arasındaki hemolitik toksisiteyi karşılaştırır. Canlılık testi ve IC değeri ve hücre canlılığı testinin hesaplanması umut verici sonuçlar göstermektedir.

Anahtar Kelimeler: Nano parçacıklar, Kanser, Lipozomlar, Gümüş nanoparçacıklar, İlaç Taşıyıcı

EXPANDED ABSTRACT

In the modern world that we live in is one of the most life threatening era. Among various deadly diseases cancer is also one of chronic disease. There are different types of cancer but Lung cancer is the most frequent malignancy in men worldwide (1.2 million new cases annually,16.7% in all cancer types). The expected incidence rates in women are usually lower (583,000 newcases annually, 8.7% in all cancer types). It is due to the aforementioned reasons the treatment of cancer is becoming a necessity and cannot be done through conventional means because although there are a number of chemotherapeutic agents available in the market which are prescribed and used for its treatment, but their weakness is that they are unable to differentiate between the targeted cells and the healthy cells and also they have shorter lifespan in the body of cancer patients and their progressive use produces undesirable toxic side effects in the healthy tissues. Thus in light of the above factors there is a great need for the development of novel drug delivery systems which are target specific, increase the lifespan of the drug, reduces the dose of drug required to produce the desired effect and also the vector used for carrying the drug should itself be biodegradable and nontoxic to the body of the patient and most importantly it should not have any sort of side effect in the body of the patients. The above stated qualities in a drug delivery can be achieved by using nanotechnology, for its offers the wide range of materials which provide biodegradability, targeted drug delivery, minimal doses and increased lifespan of drug in the body, examples of such functional systems are liposomes, conjugated metal nanoparticles, solid lipid nanoparticles etc. Amongst all the types of nanoparticles that can be used for drug delivery, liposomes when hybridized with conjugated metal nanoparticles can prove to be an efficient drug delivery system because it can provide very useful properties such as high surface to volume ratios, reduced adverse reactions and nanosized modifications.

Liposomes are the simplest artificially synthesized biological nanoparticles which have the ability to decrease the toxicity of the antitumor, antiviral and antibiotic drugs and are being introduced into clinical use and some are well underway in clinical and pre-clinical trials.

So, our aim to conduct this research was To design and implement a novel drug delivery system which would be able to selectively target cancer cells, be able to release the drug slowly and on the target site. To design a treatment which would be without or with minimal side effects to the cancer patients. To prepare Silver Nano particles and encapsulation methodology was adopted as described by Rengan et al.(2014) and after completing this step in-vitro cell line study was performed. Following steps were performed to prepare and analyze the nanoparticles:

Silver nanoparticles were synthesized and drug L24 was loaded into these particles by using a chemical method. These Drug + Silver nanoparticles were characterized. The nanoparticles were encapsulated by lipids and cholesterol using Rengan's method. The drug concentration after the formation of liposome nanoparticles was measured in the supernatant using UV-Spectroscopy. In-vitro drug release ability in cell line A549 and BEAS2B was studied and then cytotoxicity was measured by using the MTT assay.

We had three different substances, L24 (Cancer drug), Ag (Silver) and Ag-L24 (Drug and silver nanaoparticles. When we checked IC50 and cell viability then drug in encapsulation showed much better results as compared to Drug L24 and Ag alone. So, our reasearch proved that if we will use liposomal silver nanoparticles as a cancer drug carrier then it will not only minimize the side effects of drugs use against cancer before but also will show much better results.

ACKNOWLEDGEMENT

There are no words that can be found to praise and thank Allah who provided me with the opportunity and strength to accomplish this work. I sincerely thanks to my family and teachers for supporting me throughout the Master's degree. I express my appreciation and gratefulness to my honourable supervisor Dr. Yasemin Saygıdeğer, and her guidance throughout the preparation of this thesis and research project, I am also thankful to respected Assistant Professor Doğan Kaya for their contribution in nanotechnology part of my research thesis and other teachers for their support and guidance during the study period and special gratitude to my fellows and other classmates for bringing valuable ideas and corrections in this report. I acknowledge Dr. Burcu Saygıdeğer for their valuable and relevant guidance in experimentation and the analysis of data collection for writing.

Syed Hamza Zaffar Bukhari

TABLE OF CONTENTS **PAGE**

LIST OF TABLES **PAGE**

LIST OF FIGURES **PAGE**

LIST OF SYMBOLS AND ABBREVIATONS

AgNps : Silver Nano Particles

A-549 : lung carcinoma epithelial cells that constitute a cell line

Beas2B : an epithelial cell line that was isolated from normal human bronchial epithelium

MTT : (3-(4, 5-dimethylthiazolyl-2)-2, 5-diphenyltetrazolium bromide) assay

FTIR : Fourier Transform Infrared Spectroscopy

X-RD : X-ray diffraction analysis

1. INTRODUCTION

Cancer is the most challenging disease in present world. It is actually characterized by mutated cells with uncontrollable multiplication. In a process known as metastasis it is spread into different organs. Radiotherapy, Chemotherapy and surgery are conventional methods that are used to treat cancer (Xuan Wang *et al*., 2019). Despite the advancement in these techniques, chances of survival of patient are low while incidence of adverse effects of these techniques are very high. The hydrophobic nature of many chemotherapy medicines makes them less biocompatible, requiring very high concentrations to have the intended therapeutic effects. Additionally, limited solubility decreases drug absorption and excessive dosage results in high systemic toxicity. (Urvi H.Gala *et al*., 2020). Many anticancer drugs have poor water solubility by nature for two main causes. First, during the identification of new anticancer drugs, insufficient attention is usually given to the physicochemical features of drug candidates. Second, anticancer drug permeability, activity, and stability depend on specific hydrophobic structural properties, which give the drug a poor water solubility.The drugs used in chemotherapy have low specificity and also cause damaging of healthy tissues. In this sense, target oriented drug delivery system based on controlled release can be alternative of chemotherapy and other conventional techniques that have some limitations. For these limitations nanotechnology could be the solution (Navya P.N *et al*., 2019)

Nanotechnology troubleshoots one of the major problems in oncology, treatment of diseases, pharmaceutical industries, i.e., poor solubility of drugs. Poor solubility of drugs decreases the bioavailability, and increases the systemic toxicity in vivo. Nanocarriers such as silver nanoparticles, liposomes, dendrimers, gold nanoparticles and polymeric micelles not only overcome this problem but also offer additional advantages such as targeted drug delivery. Integration of

nanotechnology with other techniques like microfluidics holds great promises in the field of diagnosis (Navya P.N *et al*., 2019).

1.1. Applications of Nanoparticles:

Nanoparticles are utilized in a diversity of biotechnological and medicinal applications. With the advancement of nanotechnology, the usage of nanomaterials and nanoparticles as drug carriers has risen. When it comes to the body's ability to absorb cancer treatments, nanoparticles are absolutely essential. Usually, two- or three-dimensional nanoparticles with particle sizes between one and one hundred nanometers (nm) are employed. In the literature, iron-gold-silver nanoparticles are employed to carry cancer medications. simply because they are safe for the body and their functional groups target cancer cells. Nano-based methods offer ways for sustained drug release, enabling targeted targeting of cancerous tissues/cells, and improve transport across biological barriers. Utilizing organic, inorganic, lipid, and protein biomolecules that really are typically in the range of 1-100 nm, a broad range of nanomaterials have already been produced by carefully adjusting the chemical composition, size, and shape (morphology), which can regulate the properties and functions of the nanomaterials. Numerous anticancer medicines are delivered via these nanoparticles. In example, there are numerous advantages to using nanocarriers for drug delivery; I it can get around issues with the solubility and stability of anticancer drugs; and (ii) it can be used to design materials that can revolutionize drug delivery methods and change the pharmacological landscape of cancer treatment. (ii) prolongs the drug's half-life in the circulatory system and protects it from degradation by proteases and other enzymes; (iii) enhances drug targeting and distribution; (iv) helps the drug's prolonged release by concentrating on the cancer sites; and (v) makes it easier to distribute several treatments, which lowers the risk of drug resistance. As a result, nanotechnology is opening up new possibilities for developing materials that could alter drug delivery methods and the

pharmacological landscape of cancer treatment (Navya P.N., *et al*., 2016; Wicki *et al*., 2015).

1.2. Effectiveness of Nanoparticles:

The effectiveness of anticancer medications is well known to be significantly diminished by the time the drug reaches the target, which can make the treatment ineffective and increase off-target consequences. Only when the drug is supplied at the right dosage and exhibits maximum activity in the cancer cells will anticancer treatment programs be effective. As a result, the potential toxicity toward healthy cells should be reduced by the capacity of the nanomaterials utilized to target tumor cells to increase local concentrations of the medications in and around tumor cells. Both active and passive targeting are two types of effective nanomaterial delivery to targeted tissues (Du, W *et al*., 2015). Active targeting selectivity and payload transport capability are two key components required to maximize the efficacy and durability of nanoparticle-based active targeted systems in in vivo situations. The effectiveness of the interaction involving ligand-conjugated nanoparticles and respective target molecules is referred to as specificity, and it is weighed against any off-target effects that occur before the target molecules are reached. The interactions that arise during the biodistribution process largely determine this uniqueness. The buildup of smaller connections, which are supplied by numerous complex biomolecules based on van der Waals interactions, can hinder a nanoparticle's potential to reach its target sites. Similar to this, several smaller proteins and intrinsic biomolecules bind in an in vivo environment. sometimes referred to as Vroman's effect, occurs randomly on the surface of nanoparticles and alters the "identity" of the entire nanosystem. This modification might make nanoparticles less selective, which would result in less-than-ideal localisation at cellular targets or in targeted places. Biodistribution profile is essential to the effective operation of actively-targeted nanosystems

because they need to be close to the target areas to home in and carry out their tasks (Navya P.N *et al*., 2019).

The effectiveness of drug packaging and the programming of drug release mechanisms into the nanosystems determine the payload delivery capability. Effective drug "packing" depends on how well the drug is encapsulated or conjugated. As discussed later in the section, various nanoparticles offer various ways of trapping pharmacological molecules. The rate of medication release must be changed in response to an activation signal in order to achieve controlled release goals and sustain an acceptable therapeutic dosage over time. Open-loop control systems and closed-loop control systems are two categories of nano-systems based on which activating events cause medication release (Son, G. H *et al*., 2017). In open-loop control systems, the release of drugs is regulated by external forces like magnetic pulses, thermal pulses, acoustic pulses, or electric fields. In contrast, the existence and strength of internal cues close to the target areas in closed-loop systems regulates the pace at which drugs are released. Some modern approaches depend on the "chemistry" built into nanosystems that respond to pH or temperature, erosion brought on by the surrounding chemical environment, releasing dependent on redox reactions, and enzyme-mediated release (Prasanna, A *et al*., 2018)

1.3. Different types of nanoparticles:

It takes a lot of work to create highly effective nanocarriers that are suitable for use as medication delivery vehicles. Nanocarriers have already been created using a wide variety of materials. The primary engineering criteria for these nanoparticles as drug delivery platforms for sustained release are their size, shape, composition, surface charge, and biocompatibility. The adherence to cells, their interaction, and accumulation are influenced by the physicochemical features of nanomaterials, which can have beneficial or harmful consequences (Kaphle, A *et al*., 2018). Liposomes were the first nanoparticles to be employed in medicine

when it was originally published in 1965. In liposomes, spherical vesicles, an interior water solution is surrounded by a lipid bilayer of either synthetic or natural phospholipids. The shape of liposomes can be altered to encapsulate hydrophobic or hydrophilic drugs or other small molecules in the lipid bilayer or aqueous core, respectively. Drug delivery methods based on liposomes have been created to extend the time that medications are in circulation and lessen their toxicity to nearby healthy tissues. Consequently, these vehicles also have a number of other benefits, including that of high drug cargo loading, self-assembly, and biocompatibility. Because of their physical similarity to biological membranes and ability to combine with a range of substances, liposomes constitute good drug-carrier systems. With the remarkable progress made in liposome biomedical applications over the past 20 years, the therapeutic index of the drugs that are encapsulated has increased (L. Sercombe *et al*., 2015).

1.4. Silver Nanoparticles:

Additionally, it has been demonstrated that silver (Ag) nanoparticles can be used as anticancer drugs to treat a variety of tumours. To deliver drugs with enhanced therapeutic characteristics, Ag nanoparticles have been used. Ag nanoparticles and phytopharmaceuticals can be employed to treat cancer as non-toxic delivery systems, photothermal agents, and contrast agents (Soni, N *et al*., 2017). AgNPs, or silver nanoparticles, are of tremendous interest because of their distinct and controlled properties. Various synthetic techniques have been put forth to create these nanoparticles, which frequently call either high temperatures, high pressures, or hazardous solvents. AgNPs could and do serve as vehicles for the effective delivery of anticancer medications with higher therapeutic index and potency, avoiding the requirement for a high dose of chemotherapy to decrease the cytotoxic effects on healthy, normal human cells (MohdAbass Sofi *et al*., 2022; Khorrami S *et al*., 2018).

The aim of this project is to develop new drug carrier system because there is a need to design a novel drug delivery system which would be able to selectively target cancer cells, able to release the drug slowly and on the target site. To design a treatment which would be without or with minimal side effects to the cancer patients. Our target is to combine silver nanoparticles and chemotherapeautic drug (encapsulation of silver nanoparticles on drug) and use them to check the efficacy of this system in the cancer line A549 and BEAS2B in in-vitro conditions.

2. LITERATURE REVIEW

Cancer is a fatal disease that causes abnormal and uncontrollable proliferation of cancerous cells. The invasion of healthy tissues and organs by these unregulated cells might result in unfavorable growth and reactions that ultimately cause the organs and tissues to die. Worldwide, 3.4 million individuals pass away from cancer every year. Some of the well-known causes of cancer disease include smoking, ovarian cancer, being overweight or obese (linked to 13 different types of cancer, including breast, kidney, womb, and bowel cancers), eating processed meat, radiation (which causes skin cancer), family history, stress, environmental factors, and chance (Ferlay *et al*., 2015). Breast cancer, which accounts for 14% of all cancer-related deaths in women, is the most common type of cancer among women globally and the leading cause of death from cancer in women (Fitzmaurice *et al.,* 2015). Radiation therapy, chemotherapy, and surgical removal of solid tumors are the first-line cancer treatments. Since only a small portion of the drug concentration reaches the tumor site, the main clinical failure of chemotherapy in the treatment of cancer is regarded to be the systemic administration of the free medication. Chemotherapy's majority of active pharmaceutical ingredients (APIs) are exceedingly harmful to both healthy and malignant cells (Tao, J *et al*., 2016)

Cancer treatment continues to be quite difficult. However, in the recent several decades, there has been a significant advancement in the discovery and development of anticancer drugs. Due to problems with anticancer medication delivery, this advancement has only produced a small number of oncology medicines that are truly successful. The most popular method of administering anticancer medications is orally, however the vast majority of those that are currently in development and those that have received commercial approval have low water solubility that cannot be improved without sacrificing their effectiveness and stability. Anticancer medications' weak water solubility, when combined with other factors, results in subpar pharmacokinetic performance. As a result, when

taken orally, many medications have limited effectiveness and safety (Gala, U. H *et al*., 2020).

When liposomes are combined with conjugated metal nanoparticles, an effective drug delivery system can be developed. This is because the combination can result in high surface-to-volume ratios, less negative side effects, and nanoscale changes, which are all highly helpful qualities (Mudshinge *et al*., 2011). The simplest artificially created biological nanoparticles, liposomes are being used in clinical studies and some are already well along in the pre-clinical and clinical stages. They have the ability to lessen the toxicity of anticancer, antiviral, and antibiotic medications (Akbarzadeh *et al*., 2013; Fan & Zhang, 2013).

There is a higher danger of exposure to AgNP's hazardous side effects as it is used more frequently in consumer goods and pharmaceuticals. This is because AgNP may have leached into the environment. A sock coated with 1.36 mg of AgNP, as demonstrated by Benn and Westerhoff (2008), can discharge 48% of that coating into the water by just pulsating it in the water, or up to 100% in four subsequent washes. The oral, pulmonary, and cutaneous systems are AgNP entry sites. AgNP killed cells by generating reactive oxygen species (ROS), increasing DNA damage, and decreasing mitochondrial function regardless of how it entered the cell (Kang, Jung, & Lim, 2012). Because of this, continuing to utilize AgNP at these high concentrations may be dangerous in the near future.

Espinoza et al.'s description of the green synthesis technique using Aloe vera gel extract and sunshine was determined to be workable, easy to carry out, and low impact on the environment (2021). The best period for obtaining AgNPs was 30 seconds of solar exposure, which resulted in polydisperse AgNPs with acceptable diameters between 40 and 70 nm as shown in SEM and a zeta potential of -18.96 mV. FTIR spectroscopy revealed the existence of potential functional groups involved in the reduction of ionic silver, and UV-visible spectroscopy highlighted the surface plasmon resonance band, indicative of the creation of silver nanoparticles. The modified reverse phase evaporation method's liposomes had a

zeta potential of about -40 mV, an average diameter of 321 to 373 nm, and a polydispersity index of 0.2, which suggests size homogeneity. With a good encapsulation rate and increased stability, AgNPs were enclosed in liposomes containing cholesterol. In this way, it can be said that the technological development goals of silver nanoparticles enclosed in liposomes outlined in the current work were accomplished. Azeez Yusuf et al. (2017) It has been suggested that encapsulating AgNP in a liposome can increase its cytotoxicity at low doses by increasing DNA damage while suppressing ROS. Contrarily, multiple other studies have shown that ROS generation is required to produce the cytotoxic effects of AgNP. AgNP being enclosed in liposomes is thought to prevent ROS from having their undesirable side effects, enabling a higher level of cytotoxicity that would otherwise only be possible at very high doses. As a result, Lipo-AgNP may boost any potential biological activity with less adverse effects normally connected to high-dose exposures, hence reducing the necessary concentration of AgNP.

Saesoo et al. (2016) created a brand-new mucoadhesive nanocarrier with cervical cancer therapeutic potential. Quaternized N,O-oleoyl chitosan (QCS), an amphiphilic chitosan derivative, was created and produced. To create QCS-liposome, QCS was added to liposome vesicles (Lip-QCS). Lip-QCS was loaded with the model drug cisplatin. The physicochemical, mucoadhesive, and therapeutic benefits of Lip-QCS were examined, among its many other attributes. The liposome's mucoadhesive characteristics are improved by QCS-chitosan, which could lead to more effective targeting. As a component in vaginal formulations, lip-QCS has the potential to be used in the fight against cervical cancer. A hydrophobic chemotherapeutic agent like cisplatin was successfully encapsulated, and its therapeutic effects were shown in 3D cervical cancer mice. This technique helps to extend the drug retention duration by incorporating the particle into different formulations for therapeutic purposes, such as gels, pills, or films. Other benefits of this delivery system include its high intracellular internalization efficiency due to Lip-endocytosis-based QCS's mechanism of cell

entry. Even Lip-QCS is a hybrid nanocarrier made of chitosan and lipids, however lipids make up a large portion of the carrier. As a result, this mechanism is regarded as a reliable carrier in the trafficking of cells. In contrast, a polymeric-based nanocarrier made of chitosan is known to be passive when it comes to cell entrance. Second, the carrier surface becomes a site for conjugation with the targeted ligand to encourage a particular interaction between cells and nanoparticles due to the presence of an amphiphilic chitosan on the surface. This method makes it possible for Lip-QCS to function as an active targeting nanoparticle that is beneficial for cancer therapy. Finally, they suggested a cutting-edge mucoadhesive nanocarrier with the potential to treat cancer. The technique can be used in the creation of medications that are administered locally to treat diseases of the cervix or vagina.

Qian Sun et al. (2017) has demonstrated the use of silver-coated colloidosomes to encapsulate cargos. Small molecules cannot pass through the colloidosomes, which can be activated by ultrasound. Only a few of the capsules survived after 120 seconds of ultrasonic treatment, with the majority being broken up into tiny bits. We suggest the option of using the capsules to administer doxorubicin and other anticancer medications. The silver shells exhibit a low cytotoxicity for 10 capsules/cell, with a 72-hour cell viability of more than 60%. Doxorubicin, broken silver shell fragments, and the medication adhered to the capsule surfaces all kill cells when the silver shells are triggered. The effectiveness of the capsules depends on both their quantity and size.

Sreekanth et al. (2018) reported a straightforward, quick, low-cost, and environmentally acceptable green technique to produce AgNPs using ginseng's aqueous root extract. An influenza virus strain (A/PR/8) and a human cervical cancer cell line (HeLa) were both effectively toxic to the green-synthesized AgNPs. In the biological field, these produced AgNPs may therefore have a role as antiviral and anticancer medicines.

The findings of a global, phase 3, randomized, open-label trial that involved patients with metastatic pancreatic ductal adenocarcinoma and was carried out at 76 sites in 14 countries are reported by Wang-Gallam et al. (2018). The effects of irinotecan Nano liposomal formulation alone and in combination with fluorouracil (FU) and folinic acid were assessed in this trial (NAPOLI-1) (FA). The nanoliposomal irinotecan formulation with the addition of FU and FA produced a new therapeutic option by extending the lives of patients with the condition who had previously received gemcitabine-based therapy. In conclusion, liposomes present a desirable method for delivering anticancer drugs to specific locations. In addition to carrying chemotherapy medicines to their targeted site of action, these nanocarriers also improve circulation time, bioavailability, and target-site drug concentration buildup. They also shield the chemotherapeutic chemicals from the environment. Additionally, they lessen harmful side effects, which might range from a minor headache to cytotoxicity in healthy tissues. Liposomes may be surface-functionalized with a variety of biomolecules to provide the required receptor-specific targeting.

Alaa K. Othman et al. (2022) created liposomes using several surface changes in a thin film hydration approach. The three different nanocapsules, N1, N2, and N3, were made using the 1,2-dimyristoyl-sn-glycero-3-phosphocholine (DMPC), poly(diallyldimethylammonium)chloride (PDAA), polymer, and silica nanoparticles. Curcumin was completely enclosed within the liposome's core by layer-by-layer building PDDA and silica nanoparticles onto the liposome's surface. The produced nanocapsules were characterized using zeta potential, TGA, DLS, XRD, SEM, and fluorescence spectroscopy. Curiously, curcumin's fluorescence had a blue shift, and in the N1, N2, and N3 nanocapsules, the fluorescence efficiency was noticeably boosted by 25, 54, and 62 times, respectively. For various DMPC nanocapsule types, the efficiency of encapsulation, drug loading, and dietary curcumin's anticancer effects were also investigated. The release of curcumin from the liposomes was used to determine the pharmacological efficacy

of the liposomes. The results showed that the release of curcumin from the nanocapsules decreased as the number of layers at the liposomes' surface increased. Diffusion slows down as more layers are added because, according to the Higuchi model, curcumin releases slowly. More layers led to more curcumin encapsulation and increased anti-cancer activity because electrostatic interactions prevent curcumin from being released.

According to reports, the oral, pulmonary, or cutaneous routes are possible entry points for AgNP. AgNP killed cells by generating reactive oxygen species (ROS), increasing DNA damage, and decreasing mitochondrial function regardless of how it entered the cell. (Kang, Jung, & Lim, 2012). Because of this, continuing to utilise AgNP at these high concentrations may be dangerous in the near future. Ineffective delivery of AgNP to target cells may result in systemic toxicity since prolonged biodistribution of AgNP has been associated with systemic transport to various tissues, such as the spleen and liver (Xue *et al*., 2012). Therefore, developing strategies for effectively delivering low amounts of AgNP to target cells becomes important. The main obstacle to conventional anticancer medicines' use as chemotherapeutics is typically their generalised systemic actions. Encapsulating medications in a lipid bilayer for better delivery has been researched to counteract this unfavourable side effect, with encouraging findings (Sercombe *et al*., 2015). For instance, the potent anticancer drug doxorubicin prevents DNA polymerase from accessing DNA by blocking topoisomerase II. Doxorubicin is a highly efficient cancer treatment, but it is only occasionally used due of its unfavourable side effects, which include alopecia, hepatotoxicity, cardiotoxicity, and nephrotoxicity. (2013) Tacar, Sriamornsak, and Dass. However, doxorubicin liposomal encapsulation has been demonstrated to enhance its transport in addition to reducing the drug's unfavourable side effects, lowering the concentration necessary to cause cell death (Brown & Khan, 2012; Camacho *et al*., 2016; Souto *et al*., 2016).

Sarah D. Brown et al. (2010) have improved drug delivery by tethering the active ingredient of the anticancer medicine oxaliplatin to a gold nanoparticle. Unadorned gold nanoparticles were functionalized by coating them with a carboxylate group on top of a thiolated PEG monolayer. [Pt(1R,2R-diaminocyclohexane)(H2O)2] 2NO3 was added to the PEG surface to form a supramolecular combination with 280 (or roughly 20) drug molecules per nanoparticle. The platinum-tethered nanoparticles were examined for cytotoxicity, drug absorption, and localization in the colon cancer cell lines HCT116, HCT15, HT29, and RKO, as well as in the A549 lung epithelial cancer cell line. This entails producing gold particles with a range of sizes (20–100 nm) on which to attach the drugs, linkers with a range of lengths and structures, including terminal end groups like dicarboxylates or even thiols, the use of a variety of drugs, such as cisplatin and multinuclear drugs like BBR3464, and the addition of active targeting groups like folate and estrogen, prostate or leukemia targeting apt In all cell lines, the cytotoxicity of the platinum-tethered nanoparticles was on par with or greater than that of oxaliplatin administered alone. They also demonstrated a remarkable ability to infiltrate the nucleus of lung cancer cells. This true nanomedicine-based approach gives a novel perspective on cancer therapy and has the potential to significantly advance cancer treatment and illness management in the future.

Multifunctional nanomedicines with high drug loading capacity, flexible drug release, and real-time self-monitoring are attracting more and more interest due to their potential to improve the efficacy of cancer therapy. Here, folic acid (FA), isoreticular metal organic frameworks (IRMOF-3), and detachable polyethylene glycol (PEG) were used to produce and modify a brand-new class of Fe3O4C-based nanoparticles in a cancer microenvironment. Fe3O4C was made into a core-shell structure using a one-pot solvothermal reaction, and IRMOF-3 layers were added to the material's outer shell through layer-by-layer coating. On the surface of the nanoparticles, the FA and PEG were conjugated by reacting with the amine groups that IRMOF-3 provided. The as-produced nanoparticles

displayed a persistent photothermal effect, superparamagnetic properties, and blue fluorescence under 360 nm illumination. The in vitro experiments showed that the drug-loaded nanoparticles had a pH-dependent drug release feature, and PEGylation was effective in limiting burst drug release (only 8.0% of the medicines were released within 95 hours). The results of the confocal laser scanning microscope investigation demonstrated that FA modification can significantly enhance cell internalisation and that the nanoparticles as generated may operate as a cell imaging agent. While the IRMOF-3 modified nanoparticles showed minimal cytotoxicity in vitro, the drug-loaded nanoparticles showed pH/photothermal-stimuli enhanced cytotoxicity. There is a lot of potential for imaging-guided drug delivery and cancer treatment with the current smart drug delivery technology (Yanhong Xu *et al*., 2019)

JinjinShi et al.(2014) have developed one of the most efficient treatments for a number of cancers, doxorubicin (DOX), was used as the standard drug and linked to GOAg via ester linkages with a very high drug-loading efficiency (82.0%, weight ratio of DOX/GOAg). Next, GOAg-DOX was functionalized by DSPE-PEG2000-NGR, providing GOAg-DOX with an active tumor-targeting capacity. The release patterns of DOX from GOAg-DOX-NGR were shown to be significantly influenced by the near-infrared (NIR) laser and the SPR effect of Ag nanoparticles. In an in vivo mouse tumour model, GOAg-DOX-NGR offered much better anticancer activity without apparent detrimental effects to normal organs when compared to free DOX due to 8.4-fold higher tumor DOX uptake and 1.7-fold higher DOX released in tumor utilizing NIR laser than the other tissues. The treatment efficacy in this study was greatly increased by the GOAg-DOX-NGR nanoparticles' capacity to combine local targeted chemotherapy with exterior photothermal therapy (PTT). Additionally, GOAg-DOX-NGR worked well for photothermal ablation of tumors in addition to being a potent X-ray contrast agent for tumour diagnosis. Because of its effective chemophotothermal therapeutic efficacy, tumor-targeting feature, NIR laser-controlled drug release function, and

X-ray imaging capabilities, GOAg-DOX-NGR has a significant promise for the detection and treatment of cancer.

Multifunctional nanoparticles that may deliver extended circulation and particular accumulation, illuminate the targeted object, and intelligently dose the problematic zones will enable significant advancements in detection and treatment. To enable simultaneous tumor-cell imaging and suitable local distribution to the tumor location, we design core-shell structured hybrid nanogels (40–80 nm) with an Ag nanoparticle (NP) at their core and a smart gel made of poly(N–isopropylacrylamide–co–acrylic acid) at their shell. The pH-induced shrinkage of the nanogel, which also increases UV-vis absorption, causes the surface plasmon bands of the Ag NP core to undergo a blue shift. The smart nanogel can illuminate the mouse melanoma B16F10 cells, including the nuclear regions, by piercing cellular barriers and entering the intracellular environment. The interactions between the surface properties and concentrations of the hybrid nanogels result in various cell morphology and selective cell labelling. The pH-responsive hybrid nanogels not only have a high drug loading capacity but also exhibit a pH-controllable drug release behaviour. There are numerous potential biomedical applications for intelligent hybrid nanogels with optical and therapeutic capabilities that were produced by combining functional building blocks (Weitai Wu *et al*., 2010)

Ergang Liu et al. (2018) introduced the dual functional system that is based on dextrin-coated iron oxide nanoparticles and cell penetrating peptide (Tat) nanoparticles to produce Ag-Fe3O4 nanocomposites (Tat-FeAgNPs). To load medications, 3-mercaptopropanohydrazide, a linker containing -SH, was developed and produced. Doxorubicin (Dox) may therefore be loaded onto the silver carriers and released in a pH-dependent way. The efficiency of this system's administration was evaluated in vitro using MCF-7 cells, and it was evaluated in vivo using null BalB/c mice that had MCF-7 xenograft tumours. Our results demonstrated that doxorubicin-loaded nanoparticle cytotoxicity was enhanced by Tat and an external

magnetic field, respectively. Tat-FeAgNP-IC50 Dox's was determined to be 0.63 mol/L. The in vivo transport efficiency of Tat-FeAgNP delivering Cy5 to the mouse tumour was investigated using in vivo optical imaging assays. The most efficient accumulation in the tumour was created by Tat-FeAgNP-Cy5 (6.72.4% ID of Tat-FeAgNPs). The strongest tumor-inhibiting effects were likewise demonstrated by Tat-FeAgNP-Dox, which significantly reduced the tumor's specific growth rate by 29.6% (P = 0.009). This was most likely because it had better tumour drug delivery capacities than the control nanovehicles. Given the rapid development of artificial nanomaterials for various uses, in vivo toxicological studies are urgently required to evaluate the potential adverse effects of nanomaterials on the environment and human safety. Zebrafish have long been recognised as the "gold standard" for biosafety investigations of pesticides and pollutants due to their high fecundity, affordability, precisely defined developmental stages, optical transparency, and other qualities. For high-throughput nanotoxicity testing, zebrafish offers a lot of potential. These nanomaterials' physicochemical properties, such as size, surface charge, and surface chemistry, affect their biosafety in zebrafish in vivo toxicological profiles. Examples include Ag nanoparticles (NPs), CuO NPs, silica NPs, polymeric NPs, quantum dots, and nanoscale metal-organic frameworks. Zebrafish are employed in our research to highlight recent advances in the in vivo delivery of nanopharmaceuticals as a model organism for therapeutic evaluation, biodistribution tracking, and the controlled release of loaded drugs. The limitations and special problems of the zebrafish model are also explored. In general, it is envisaged that zebrafish will serve as a high-throughput screening platform for the assessment of nanotoxicity and drug delivery, which may offer recommendations for the creation of risk-free nanomaterials and more potent nanomedicines (Hao-RanJia *et al*., 2019).

The Monireh Rasoulzadehzalia & HassanNamaz (2018) publication describes the straightforward synthesis of novel pH-sensitive bio-nanocomposite

hydrogel beads based on chitosan (CH) and GO-Ag nanohybrid particles for the controlled release of anti-cancer drugs like doxorubicin (DOX). The UV-vis loading efficiency of doxorubicin into test beads was shown to be high utilising UV-vis spectroscopic analysis. On the GO sheets, the structural characteristics and the generation of silver nanoparticles were evaluated using FT-IR, TEM, XRD, and SEM techniques. Additionally, the antibacterial activity, swelling, and drug release profiles of the created nanocomposite beads were evaluated. An in vitro drug release test was also used to assess the potency of CH/GO-Ag nanocomposite hydrogel beads as a drug carrier for the controlled release of anti-cancer drugs like doxorubicin (DOX). A more controlled and sustained drug release profile was seen for CH/GO-Ag nanocomposite hydrogel beads, and this was enhanced by including more GO-Ag nanohybrid particles.

3. MATERIAL AND METHODS

Silver nano particle was synthesized by using chemical method and their characterization was done by Transmission Electron Microscope (TEM) and Scanning Electron Microscope (SEM).

3.1. Materials:

Sodium borohydride (NaBH4) (MERCK—106,398) [, NaOH (MERCK—1.064.621.000), and Silver nitrate Ag(NO3) (Aromel kimyamedikal—2318539) Sodium citrate dihydrate (99%) (MERCK—1.064.321.000), 3-(4, 5-dimethyl-2-thiazolyl)-2, 5-diphenyltetrazolium bromide (MTT) (BioFrox), fetal bovine serum (FBS) (HyClone—SV30160.03), DMSO (Sigma—D.5879), Acetone, Ethanol (AMRESCO—193C427), Chloroform, Petroleum Ether (Sigma- Aldrich—V) , Round bottom three necked flask, RPMI, Trypsin (Hyclone—SH30042.01), Dichloro-dihydro-fluorescein diacetate (DCFH-DA), Dulbecco's Modified Eagles Medium (DMEM) (Hyclone—SH30081.01) and the solvents, analytical grade ethanol (95%), chloroform(98%) and toluene (99.7%), Distearoyl phosphatidylcholine (DSPC) , Cholesterol, L24, Glassware, A549 cell line, BEAS 2B. 96 wells MTT plates. Hot/Strring plate, Dynamic light scattering, UV-VIS Spectrophotometer.

Table 3.1. Name and catalogue number of chemicals.

Chemical	Company	Catalogue Number
Sodium borohydride (NaBH4)	MERCK	106,39
Sodium Hydroxide (NaOH)	MERCK	1.064.621.000
Silver Nitrate AgNo3	Aromel kimyamedikal	2318539
Sodium citrate dihydrate	MERCK	1.064.321.000
Fetal bovine serum (FBS) (H3	HyClone	SV30160.03
DMSO	Sigma	D.5879
Ethanol	AMRESCO	193C427
Petroleum Ether	Sigma-Aldrich	V
Trypsin	Hyclone	SH30042.01
DMEM	Hyclone	SH30081.01
Cholesterol	(Source- Egg)	
Acetone	Sigma	439126
Choloroform	Sigma	1.02445
RPMI	Sigma	R4130
Ethanol	Sigma	493511
Toluene	Sigma	244511

3.2. Methodology:

To prepare Silver Nano particles and encapsulation methodology was adopted as described by Rengan et al.(2014) and after completing this step in-vitro cell line study was performed according to Manivasagen et al. (2016). Following steps are performed to prepare and analyze the nanoparticles:

- Silver nanoparticles were synthesized and drug L24 was loaded into these particles by using a chemical method.
- These Drug + Silver nanoparticles were characterized.

- The nanoparticles were encapsulated by lipids and cholesterol using Rengan's method.
- The drug concentration after the formation of liposome nanoparticles was measured in the supernatant using UV-Spectroscopy.
- In-vitro drug release ability in cell line A549 and BEAS2B was studied and then cytotoxicity was measured by using the MTT assay.

3.2.1. Synthesis of Silver Nanoparticles:

Chemical Equation of synthesis.

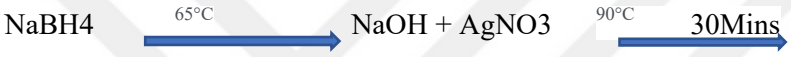

Using sodium borohydride to reduce silver nitrate is one of the most common ways to make silver nanoparticles. Both the reduction of the ionic silver and the stabilization of the created nanoparticles require a significant excess of sodium borohydride.

- 0.157g of AgNO3 was dissolved to 10ml of DMSO (Sonication)
- 0.701g of NaBH4 was dissolved to 35ml of DMSO
- 0.5562g of NaOH was dissolved to 35ml of DMSO (Sonication)

A three-necked round bottom flask was filled with 35ml of ultra-pure water and 0.707g of sodium borohydride (NaBH4). The three-necked round bottom was set on a stir plate with a magnetic stir bar added. It was stirred for about 10minutes to reach the temperature at 60°C. AgNO3 was dripped into stirring NaBH4 slowly. After the addition of this color was changed into black. When temperature was reached to 90 ^{0}C dripping of NaOH was started. When it ends colors was changed into white again. Temperature was kept maintained at 90 for 30mins.The solution

was filtered and centrifuge at 9000RPM for 6mins and this process was repeated for 3-4times.

3.2.2. Synthesis of Silver Nanoparticles & Drug loading by chemical Method:

Chemical Equation of synthesis.

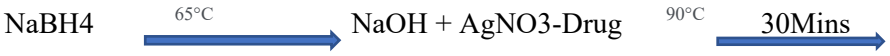

Using sodium borohydride to reduce silver nitrate is one of the most common ways to make silver nanoparticles. Both the reduction of the ionic silver and the stabilization of the created nanoparticles require a significant excess of sodium borohydride.

- 0.157g of AgNO3 was dissolved to 10ml of DMSO (Sonication)
- 0.701g of NaBH4 was dissolved to 35ml of DMSO
- 0.5562g of NaOH was dissolved to 35ml of DMSO (Sonication)
- Drug (L24) was dissolved to 15ml of DMSO (Sonication)

3.2.3. Procedure:

35ml of ultra-pure water was added along with 0.7012g of sodium borohydride (NaBH4) to a three-necked round bottom flask. The three-necked round bottom was set on a stir plate with a magnetic stir bar added. Stirred for about 10minutes to reach the temperature at 60°C. AgNO3 was dripped into stirring NaBH4 slowly. After adding this color did not change and it remains white. At the start temperature was 70°C but then we slow down the temperature that reach to 65°C at the end.

Then stirring was set at 45 and allow it to reach temperature at 80°C. AgNO3 + Drug (L24) was added into the sodium borohydride and sodium

hydroxide solution at approximately 1drop per second. It ends in 10mins. After this color of solution changed into black. Then allow it for about 30mins to keep temperature maintained at 90°C. Color of solution was changed into light brown. The solution was filtered and centrifuge at 9000RPM for 6mins and repeat this process for 3-4times.

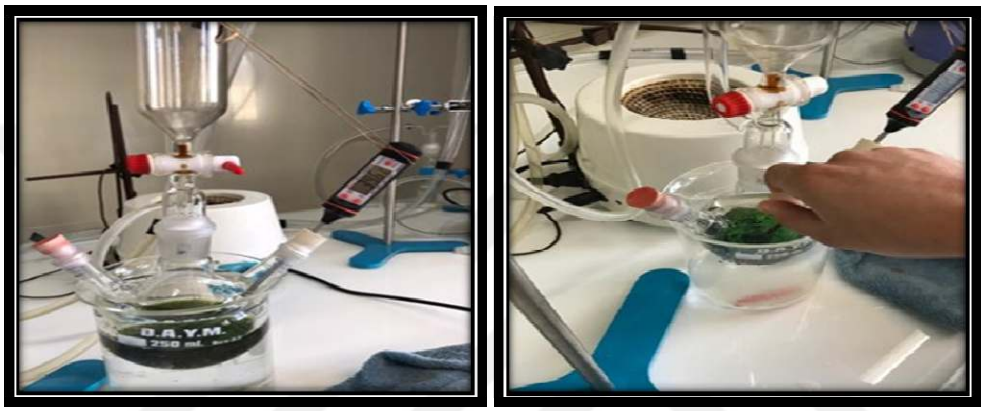

Figure 3.1. Coupling of the Ag nanoparticle and Drug L24

The solution was filtered and centrifuge at 9000RPM for 6mins and repeat this process for 3-4times.

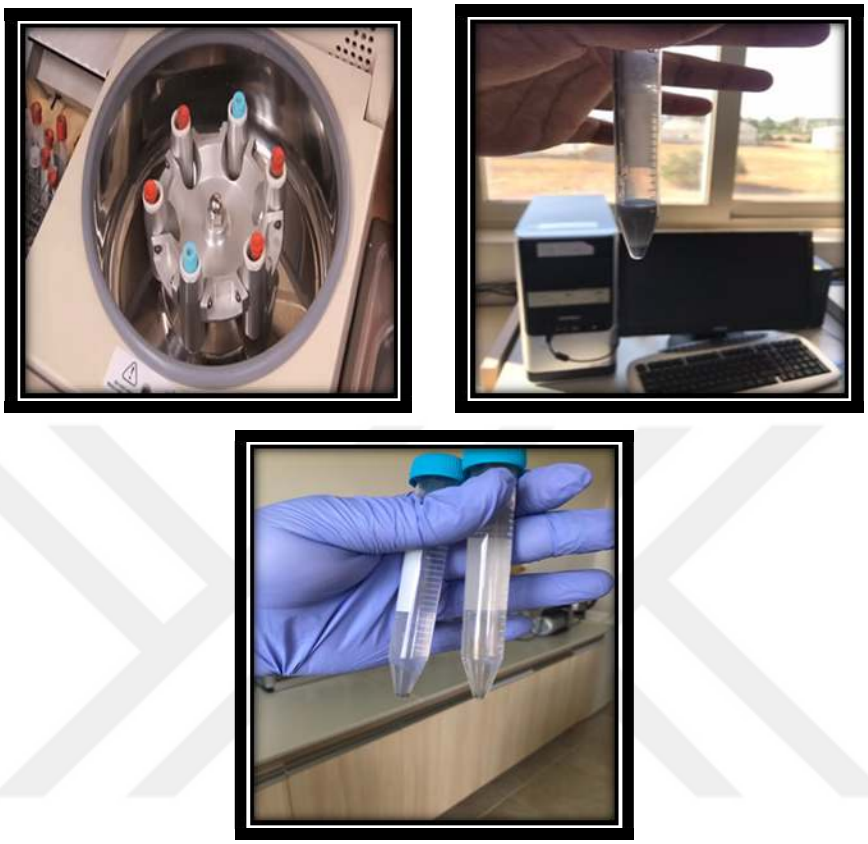

Figure 3.2. Centrifugation for the separation of Ag Nano particle from the solution.

3.2.3.1. Characterization technique

3.2.3.1.(1). FT-IR Spectroscopy

An easy way to identify the different functional groups in molecules is infrared spectroscopy; likewise, through this technique, one can find the absorption band to affirm the pure compound or to identify the accumulation of particular impurities influences. Absorption required the changing vibration and the rotation status of molecules in the infrared region. Absorption of infrared light occurs only in the infrared region. Absorption of the infrared light occurs only if the infrared energy photons cause a change in the dipole moment of that molecule in the semi-crystalline materials e.g. polymer having diverse chemical formulas. FT-IR

spectroscopy is a widely utilized method for the examination of atomic structures and synthetic chemical bonds of polymers. Of pure UHMWPE and incorporated $NiFe_2O_4$/GO into the polymer hybrid were recorded using Nicolet-6700 Fourier transform infrared spectrometer (Thermo Electron Corporation, Waltham, MA, USA), at a resolution of 6 cm^{-1} within the range of 6000 cm^{-1} to 400 cm^{-1}.

3.2.3.1.(2). FTIR protocol

Prior to analysis, AgNPs were sonicated for 5 minutes, and a drop of appropriately diluted sample was placed onto a carbon-coated copper grid. The liquid fraction was allowed to evaporate at room temperature. Fourier transform infrared (FTIR) spectral measurements were carried out to identify the potential biomolecules in cannonball leaf extract which is responsible for reducing and capping the bioreduced silver nanoparticles.

3.2.4. Methods of preparation of Liposomes

Egg yolks, which contain lecithin's that are useful for the creation of liposomes, were used as the raw material for liposome synthesis. By using the thin film hydration (Bangham) technique, liposomes were created. The process used an organic phase to dissolve the lipids, which is then removed under vacuum. The result was the formation of the thin, dry lipid film. Under agitation, the film was further hydrated, resulting in the progressive separation of lipid lamellas and the production of vesicles. Every single one of the employed extracts was dissolved in chloroform (20 mg/mL) and then put into a flask with a flat bottom. To create a thin lipid coating, the chloroform was evaporated using a rotary evaporator until it was completely dry. In a water bath at 42°C for two hours with constant rotation, the film was hydrated with an aqueous solution (4 mL of 1% PBS buffer). Two components of the obtained liposomal suspensions were separated. The first was immediately collected and contained multilamellar vesicles (MLV). The second

component formed tiny unilamellar vesicles after 15 cycles of extrusion via a 100 nm ISOPORE® membrane filter (LiposoFast by Avestin, Germany) (SUV).

3.2.4.1. Isolation of phospholipids (lecithin) from egg yolk

3.2.4.2. Materials:

- Acetone
- Fresh egg yolk
- Chloroform
- Ethanol
- Filter paper
- Bunsen burner

3.2.5. Procedure:

1. **Precipitation:** Acetone 50ml was measured and transferred into beaker containing egg yolk. After mixing acetone and egg yolk start precipitating, mixed well with glass rod and allowed it to stand for 25minutes.

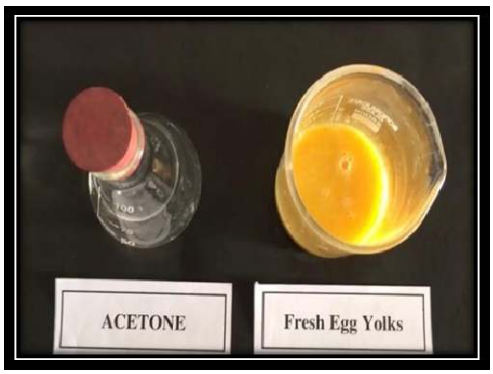

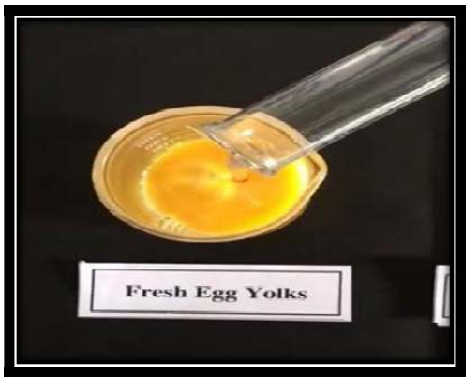

2. **Centrifugation:** Precipitated egg yolk was transferred to centrifuge tube and centrifuge it for 5 minutes at 400 rpm. Precipitated egg yolk form pellet and acetone from supernatant after centrifugation. Supernatant contained acetone was discarded.

3. **Washing-1:** Pellet of precipitated egg yolk was transferred from tube to Petri-dish. Washing was done by adding acetone to solubilize the sterile, triglycerides and other lipids.

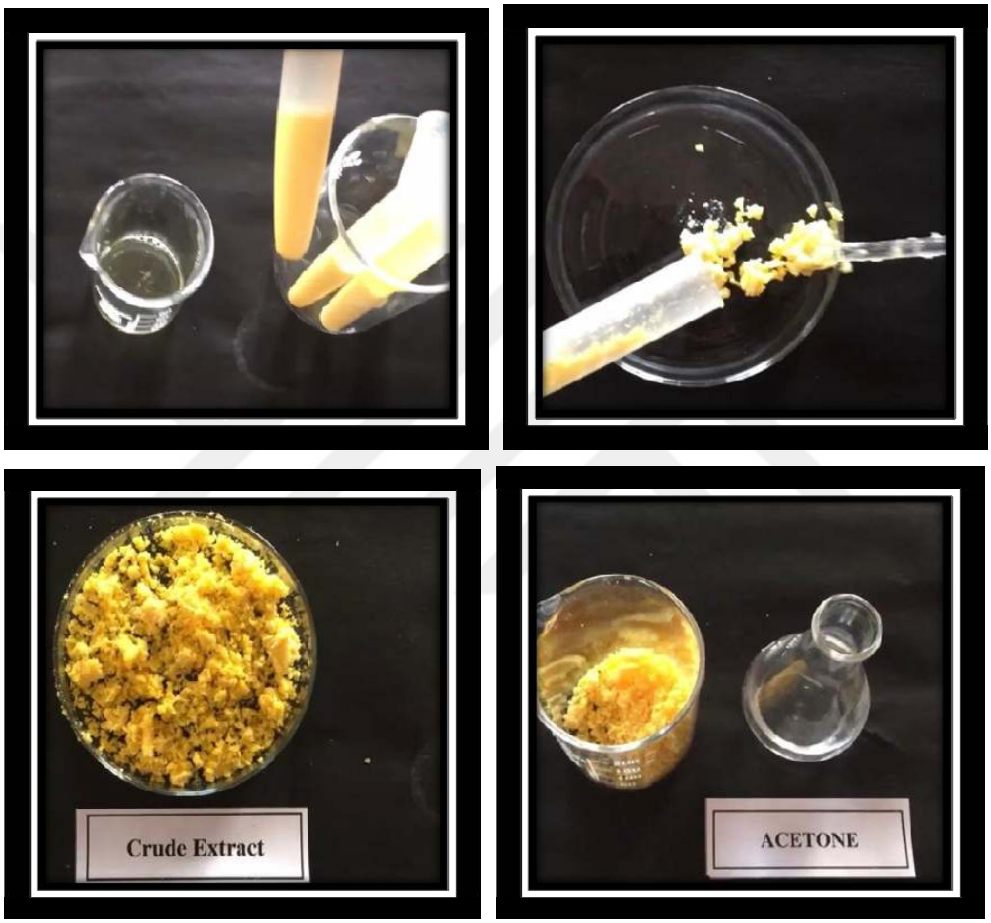

4. **Washing-2:** Content of the petri-dish was filtered by using filter paper and this filtration was repeated 3-4 times by adding acetone until filtrate becomes clear.

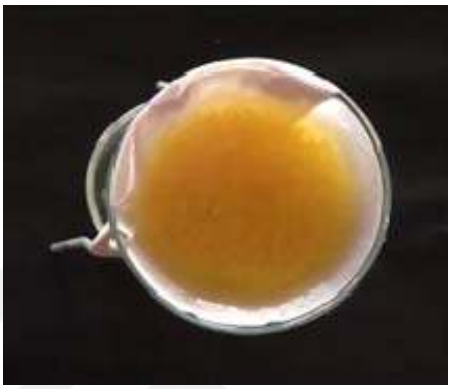

5. **Extraction of lipids:** Phospholipids was extracted from the filtrate of washed egg yolk precipitate as aforementioned. Extraction solvent chloroform and ethanol was used by the ratio of 2:1 respectively. 40ml chloroform and 20ml of ethanol was added into egg yolk washed filtrate. Well mixed and allow it to stay at room temperature for 3hr.

6. **Filtration:** After previous step, solution was filtered. Filtrate was collected into Petri dish and precipitate was discarded. Process was repeated 2-3 times with ether and acetone.

7. **Collection:** After the repeated filtration final filtrate was collected into Petri dish and stir it with glass spatula. After drying the orange red sticky substance is lecithin.

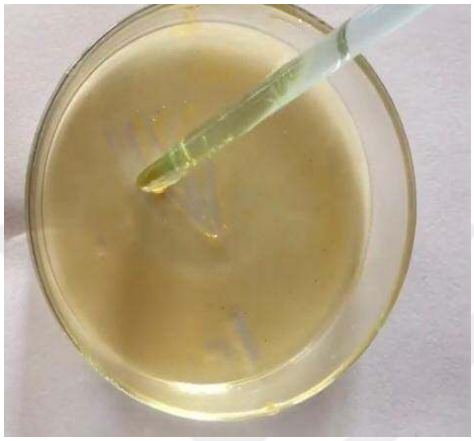

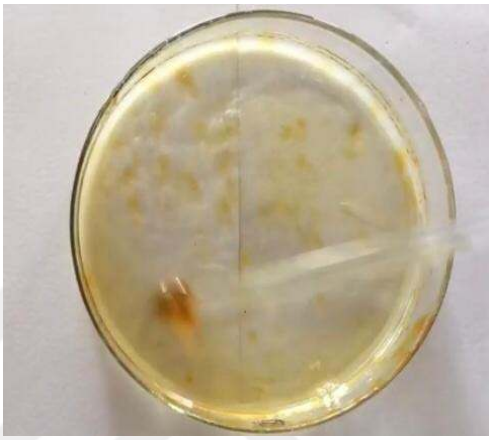

3.2.6. Encapsulation:

3.2.6.1. Materials:

Distearoyl phosphatidylcholine (DSPC)

Lecithin

Chloroform

3.2.6.2. Procedure:

Lecithin and Distearoylphosphatidylcholine (DSPC) were dissolved in 5ml of chloroform and then combined until the mixture was transparent. Then, it was overnight vacuum-dried at 52C. (above melting temperature of DPPS). The resulting lipid cake was shaken at 60 C while being rehydrated in distilled deionized water. An AgNP solution was then added after the lipid had been rehydrated, resulting in a final lipid concentration of 1 mg/ml of DPPS and 0.23 mg/ml of lecithin, giving a 7:3 molar ratio. The solution was then shaken for a

further 20 minutes at 60 degrees Celsius before being briefly vortexed and extruded via a 100 nm Nanosizer polycarbonate extruder (TTScientific, Knoxville, USA). The resulting colloidal mixture was then stored at 4 degrees Celsius before use.

3.3. Cell Culture:

Human non-tumorigenic lung epithelial cell lines (BEAS2B) and human lung alveolar carcinoma epithelial cells (A549) (we took from Gaziantep university Turkey, A549 human lungs cancer cell line derived from 56year old male patient, adenoma histologic subtype) were both cultivated at 37 degrees in a humid environment (5% CO2 + 95% air. 2 mL of trypsin-EDTA was added to a T75 flask, an inverted microscope used to check for cell layer separation. Detachment happened in 3 to 10 minutes. Cell clustering was encouraged by agitation, thus avoid agitating the cells during this phase. Cells was placed in an incubator for 5 minutes to encourage dispersion if they were not separated.

- The cells were centrifuged and the supernatant was removed to neutralize the trypsin-EDTA by adding full medium at a volume that is 4 times the volume of the trypsin-EDTA added. 6-8 mL of growth medium was added to pellet and aspirate cells with gentle pipetting.
- Aliquots of the cell suspension added to culture containers at the proper split ratio 1:5.
- Grow organisms in 5% CO2 at 37 °C. Keep the culture at 1 x 104 and 2 x 103 cells per cm2. The cell density was calculated about 7 x 104 cells/cm2 by counting the cells.
- A549 cells took around 22 hours to double. Every 4–7 days, divide a confluent A549 cell culture 1:4–1:9 with trypsin/EDTA, and replace the entire media every 2–3 days. Instead of using a culturing medium that contains 10% FBS, freeze cells in a modified DMEM mixture that contains 20% FBS and 10% DMSO for long-term storage, with a cell concentration of roughly 2 x 106 per vial.

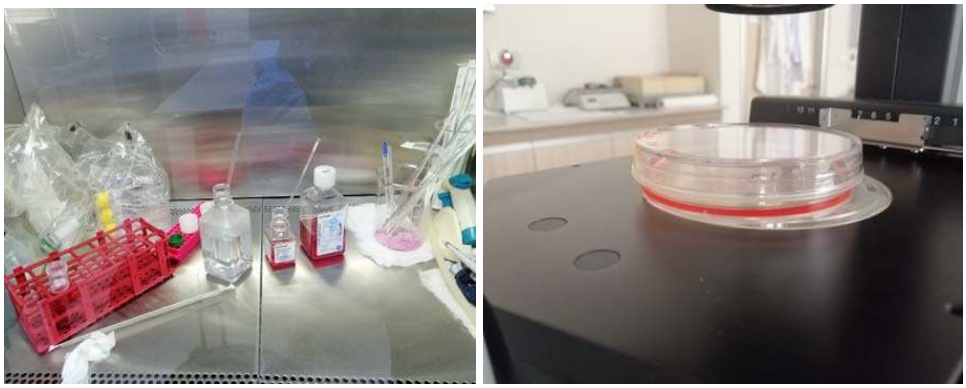

Figure 3.3. Cell culturing in the Biosafety safety cabinet

3.4. Cytotoxic Test by using MTT:

Cellular metabolic activity was assessed using the MTT test as a measure of cell viability, proliferation, and cytotoxicity. The MTT reagent can pass through the cell membrane as well as the mitochondrial inner membrane of viable cells presumably due to its positive charge as well as its lipophilic structure and is reduced to formazan by metabolically active cells. Intracellular reduction of MTT mediated by oxidoreductase and dehydrogenase enzymes and electron donors (mainly NAD(P)H) at different stages of the glycolytic pathways to the mitochondrial electron transport chain. The role of mitochondria in MTT reduction measured mitochondrial activity in viable cells.

3.4.1. MTT Assay

The MTT assay typically performed after a few hours of incubation of cells with MTT. Viable cells with active metabolism convert MTT into a purple colored formazan product with an absorbance maximum near 570 nm. When cells die, they lose the ability to convert MTT into formazan, thus color formation serves as a useful and convenient marker of only the viable cells. Subsequently, the lowering of the light transmission by absorbance and other mechanisms by the homogenized MTT-formazan solution was measured by a microplate reader in terms of its

optical density (OD) at a wavelength which MTT-derived formazan absorbs the most (around 570 nm). The measured OD values are assumed to be a representation of formazan concentration and consequently the intracellular reduction of MTT.

3.4.2. Reagent Preparation

3.4.2.1. MTT Solution

- MTT was dissolved in Dulbecco's Phosphate Buffered Saline, pH=7.4 (DPBS) to 5 mg/ml.
- Sterilize the MTT solution was filtered through a 0.2 µM filter into a sterile light protected container.Stored the MTT solution, protected from light, at 4°C for frequent use or at -20°C for long term storage.
- Ethanol was added as a solubilization solution.

3.4.2.2. MTT Assay Protocol

- The cells were Prepared and placed in 96-well plates containing a final volume of 100 µl/well.
- Incubated for 6-48 hours period of exposure.
- 10 µl MTT Solution was added per well to achieve a final concentration of 0.45 mg/ml.
- Incubated 1 to 4 hours at 37°C.
- 50 µl ethanol was added to each well to dissolve formazan crystals
- Well mixed by keeping at shaker for 15mins to ensured complete solubilization.
- Absorbance was recoded at 570 nm.

Figure 3.4. MTT Assay for cell viability in 90 wells plate

Figure 3.5. MTT Assay for cell viability for laser exposure after incubation

3.4.3. Cell Proliferation assay:

On 4 different 96-well plates, A549 Cells and BEAS2B (200000cells /200 ul) were seeded before being incubated at 37 degrees Celsius under 5% CO2 for an entire night. For each cell line, one plate with a laser and one without a laser Fresh medium containing medication, NPs, and Ag-NPs was then added to the wells in place of the previous medium. Initially, we used 32 wells for the drug, 32 for NPs, and 32 for silver NPs plus drug. Around (200ul) of a specific sample was poured to

each well, keep them in an incubator, and wait for approximately 4 hours. One MTT plate from each cell line was incubated for 24 hours after being subjected to a high intensity laser for roughly 10 minutes. (Using a high energy laser causes a greater absorption of light on the target material's surface.) Chemical bonds from the target material's surface are destroyed as a result of the rapid temperature rise.) Using the MTT assay, the effects of the nanoparticles on cell viability were evaluated. Each well of four distinct plates received 20ul of MTT solution after 24 hours, and the plates were then incubated for 4 hours. The MTT was dissolved in 98% ethanol (50ul) after the supernatant was taken off. A microplate spectrophotometer was used to test each well's absorbance at 570 nm. As a control, cells cultured with only the medication and no nanoparticles were utilized.

3.5. IC Value calculation for MTT Assay results

To calculate IC50, series of dose-response data (e.g., drug concentrations Ag, L24, Ag-L24 and Cell viability% for each) was used. The values of y were in the range of 0-1.

a) **Linear Regression**

The simplest estimate of IC50 was to plot x-y and fit the data with a straight line (linear regression). IC50 value was then estimated using the fitted line, i.e.,

$$Y = M * X + C,$$

$$IC50 = (Y-C)/M.$$

b) **Log transformation**

Frequently, linear regression is not a good fit to dose-response data. The response-curve fits better to a straight line if the x-axis is logarithm-transformed.

c) **Excel add-in**

Excel add-in for calculating IC50 values. Data was put in the table. The mean value was calculated. And then linear aggression was find out after then aforementioned formula was used to calculated the IC50 for each result.

d) **Four-Parameter Logistic Function**

Four-parameter (A, B, C, D) logistic function (or Sigmoidal)

$$y = D + \frac{A - D}{1 + 10^{(x - \log C)B}}$$

is frequently used to fit dose-response curves. The drug data x is in logarithmic form. This is a standard function in most statistics software. The parameter C is the estimate of IC50.

4. RESULT AND DISCUSSION

4.1. Characterization of Ag nanoparticles

4.1.2. FTIR Analysis:

FTIR spectroscopy used to analyze the intermolecular interaction bases on bending vibrations and stretching of various bonds within the particles. The spectrum of AG nanoparticles has been shown in Fig 7. There is a broad band observed within the range from 4010.50 cm^{-1} to 3500 cm^{-1} which is due to the O-H stretching alcoholic group. This has also been reported by Saif *et al*. There is a slight hump has been reported at 2385.52 cm^{-1} and 2115.53 cm^{-1} exhibits the (OH) group due to the presences of phenolic groups with alcohols. A very sharp absorption peak at 2115.53 $cm^{-1}$and 1919.96 cm^{-1} identified due to the stretches of C-H and O-H of carboxylic acid and alkanes surfaces. A very deep absorption at 1651.73 cm^{-1} absorption band exhibits the C=C aromatic ring stretches vibrations and C=O stretch vibrations in phenols as well. Previous studies demonstrated that the FTIR bands that occurred at 3388 cm-1, 1636 cm-1, and 1039 cm-1, respectively, are caused by the O-H/N-H, C=C, and C-O-C stretching vibrations, indicating that a colloidal suspension is responsible for the polyphenols' interaction with the silver metallic ion.

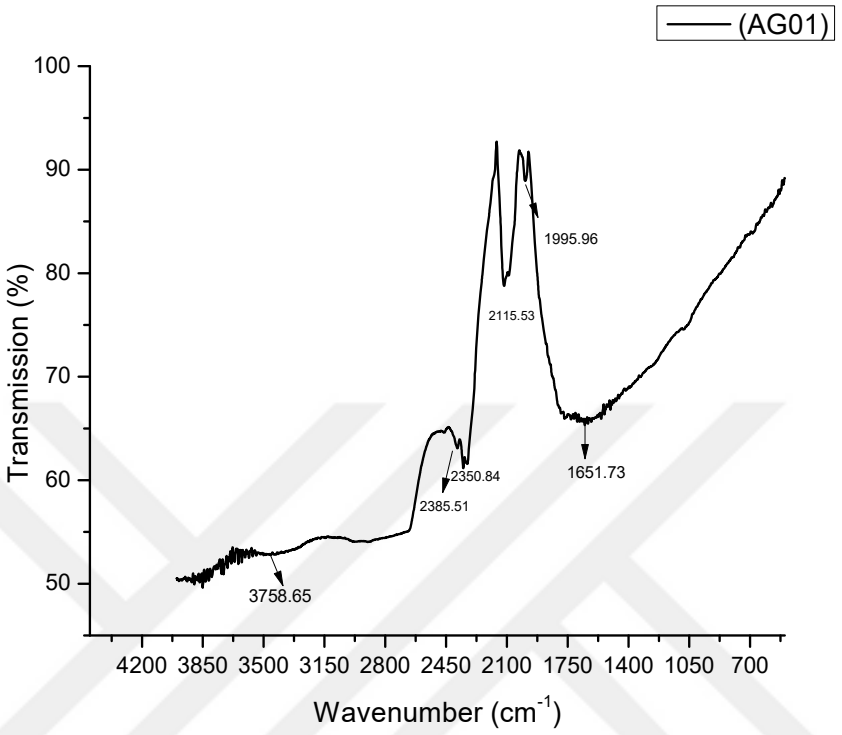

Figure 4.1. FTIR spectroscopy of AG nanoparticles

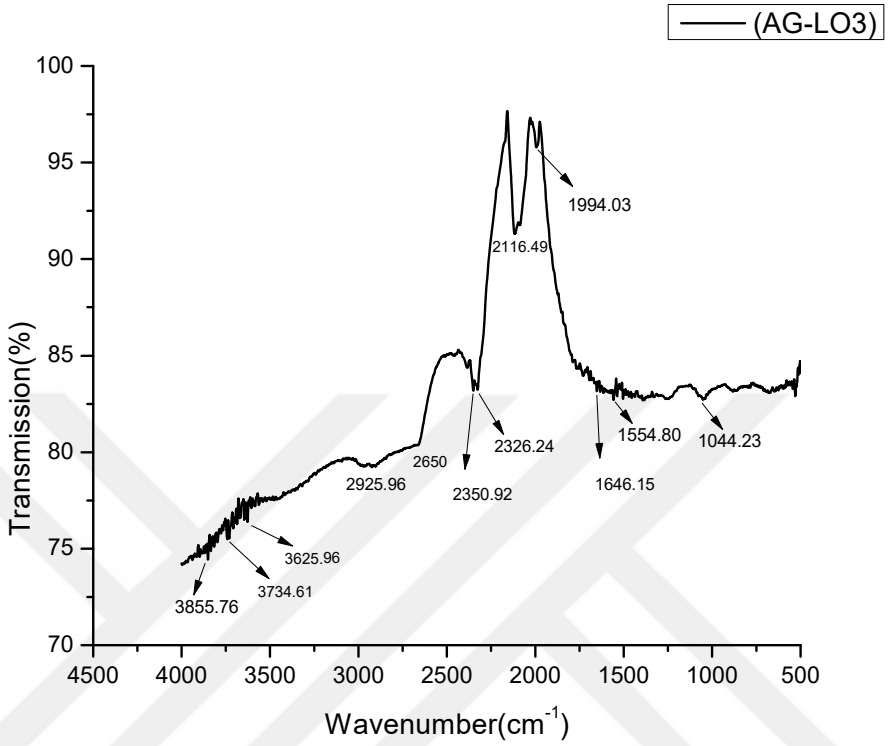

Figure 4.2. FTIR spectroscopy analysis of AG-LO3

Fig 2 shows the FTIR spectrum of Ag nanoparticles with drug loading LO3.by comparing the graph of Fig 1 and Fig it can be accompalished that tha peaks that occurred in the range of (1700-500) cm^{-1} is under the modification if Fig 2 with strong absorption. The wavenumber of the OH bending vibration at 3855 cm-1 appeared to wide and higher in intensity, as can be seen in the FTIR spectrum of Ag NPs in Figure 2. A shift from 1651 cm-1 to 1646 cm-1 was made in the peak of the C=O stretching vibration of carboxylic acid groups (see Figure7). It appears that the intensity of this band declines and shifts to 1646 cm-1 (shown in Figure 8)

4.1.3. X-ray diffraction technique (XRD)

Cu-Kα radiation with a wavelength of 1.540 Å was employed for the X-ray diffraction examination, which was carried out using BrukerAXS Germany's D-8 Discover. The device required 40 mA current and 45 kV voltage to operate well. The data was gathered at a rate of 1 degree per minute from 5 to 80 degrees. After obtaining spectra, Bragg's law was applied to determine the lattice spacing, d_{hkl}.

The investigation using X-ray diffraction was accomplished with BrukerAXS Germany(D-8 Discover)with Cu-Kα radiation having wavelength 1.540 Å, In order to perform the proper function of device, 40 mA current and 45 kV voltage was used. The rate of scanning at 1 degree/minute was used to collect the data from 5^{o}-to-80^{o}.Bragg's law was used after getting spectra for calculation of the lattice spacing d_{hkl}

$$\mathbf{d_{hkl} = n\lambda/2\sin\theta}$$

Whereas, 'λ' represent X-ray wavelength, 'n' shows diffraction level and 'θ' is the Bragg's angle.The particle size (D) can be determined by Scherrer's formula using FWHM values from XRD peaks and is given below

$$\mathbf{D = (k\,\lambda)/(\beta\cos\theta)}$$

In above relation, 'D' is the particle size and 'β' corresponds to the value of FWHM, whereas 'k' constant is called crystal factor having value of 0.94.

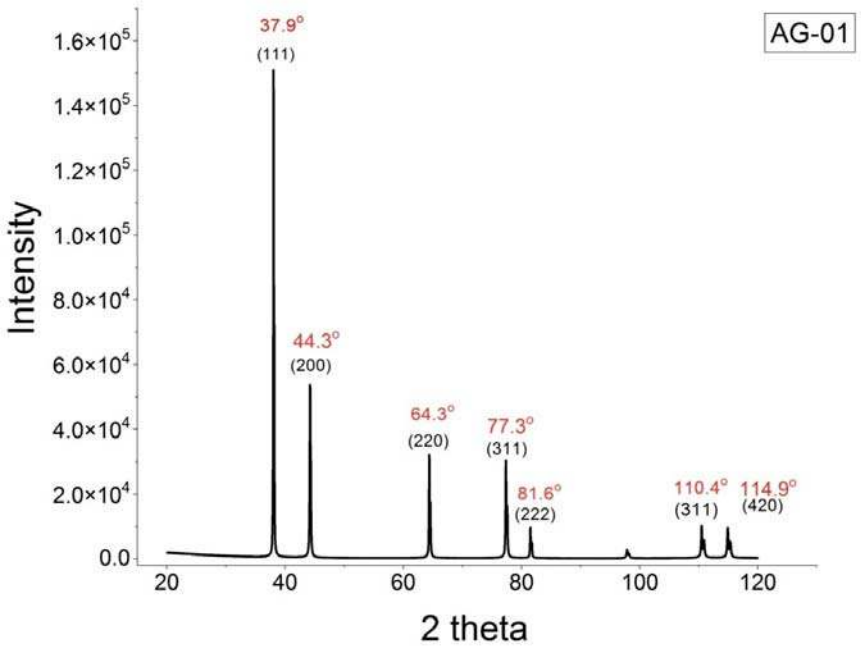

Figure 4.3. XRD data of Silver nano particles

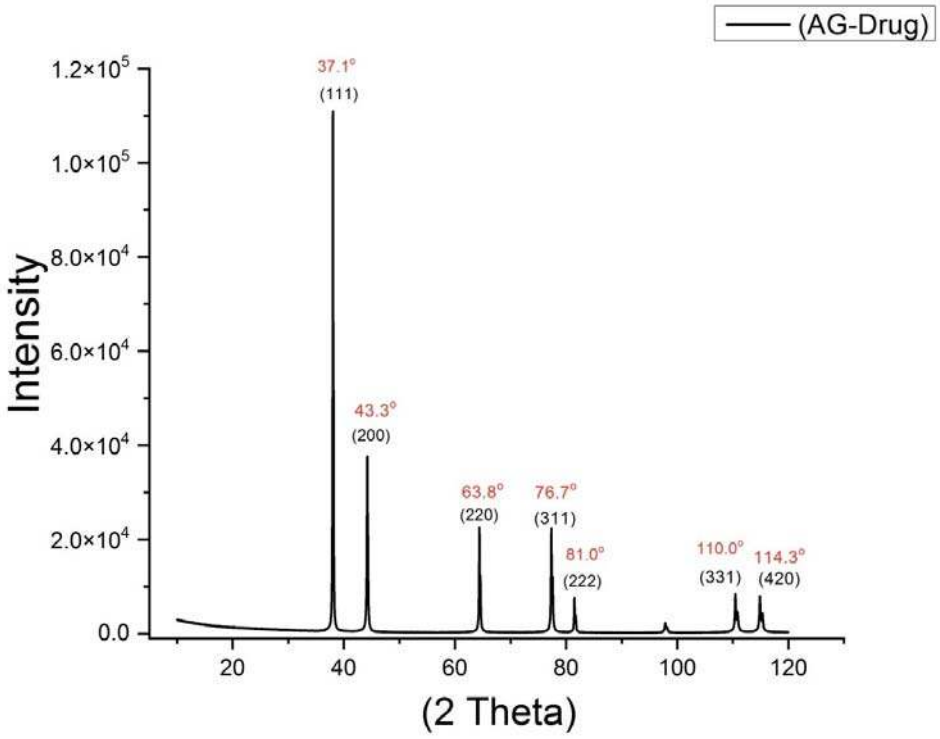

Figure 4.4. XRD data of drug coated Silver nano particles

Table 4.1. Calculated structural parameters from XRD data

Sample Code	Peak Position(2)	(HKL) Values	D (nm)	Average lattice parameter a(Å)	Inter layer spacing d(nm)	Crystallinity (%)
AG-01	37.93481	111			0.236987567	
	44.30347	200			0.204285639	
	64.32757	220			0.144696815	
	77.37228	311	62.64655	4.089395	0.123234344	61%
	81.61931	222			0.117861303	
	110.4398	331			0.093783018	
	114.9896	420			0.091336678	
AG-Drug	37.17692	111			0.241642826	
	43.34815	200			0.208563804	
	63.83139	220			0.145701426	
	76.7122	311	57.68954	4.157735	0.12412933	53%
	81.08459	222			0.118503093	
	110.0138	331			0.094026088	
	114.3961	420			0.091640311	

For structural analysis of synthesized silver nano particles is performed while using the X-ray diffraction data, which shows the standard diffraction peaks at 37.93°, 44.30°, 64.33°, 77.37°, 81.61°, corresponding to (111), (200), (220), (311), and (222) planes of pure silver, respectively .

4.2. Effects of Drug L24 and Ag Particles on A549 cancer cell line

The MTT Assay data results were obtained after the 24hr incubation of A549 cancer cell line after treating with L24 Drug, Ag nanoparticles separately and both in coupled form (Ag-L24) .the cytotoxic activity of AgNPs, L24 and Ag-L24 drug was assessed by using MTT Assay. The main purpose was to assess the effect

of AgNPs, L24 drug and the coupling effect of both Ag-L24. The laser effect was also analyzed and its effects were compared with normal treatments (Ag,L24 & Ag-L24) on A549 cancer cell line. For this purpose 570nm straight laser was used in which Cancer cell line A549 was exposed with laser for 30 seconds.

The IC value of each Normal triplet Ag,L24 & Ag-L24 treatments (without laser exposure, Ag-L24 N) are given in the table3. These IC values were calculated from IC50 value by taking the log of concentration and cell viability% of each given treatment). IC value displayed in the table 4.2 was determined by taking the log: conc. The IC50 value quantifies the amount of an inhibitory drug, substance, extract, or fraction required to inhibit a biological component by 50%. The IC value of A549 cell line was calculated for L24 was 47.66, Ag 81.11 and Ag-L24 was 6.

Table 4.2. IC value calculated from IC50 for each treatment for A549-Normal (without laser)

Number	Name of treatment	IC Value for A549-N
1	**L24**	**47.66**
2	**Ag**	**81.11**
3	**Ag-L24**	**6**

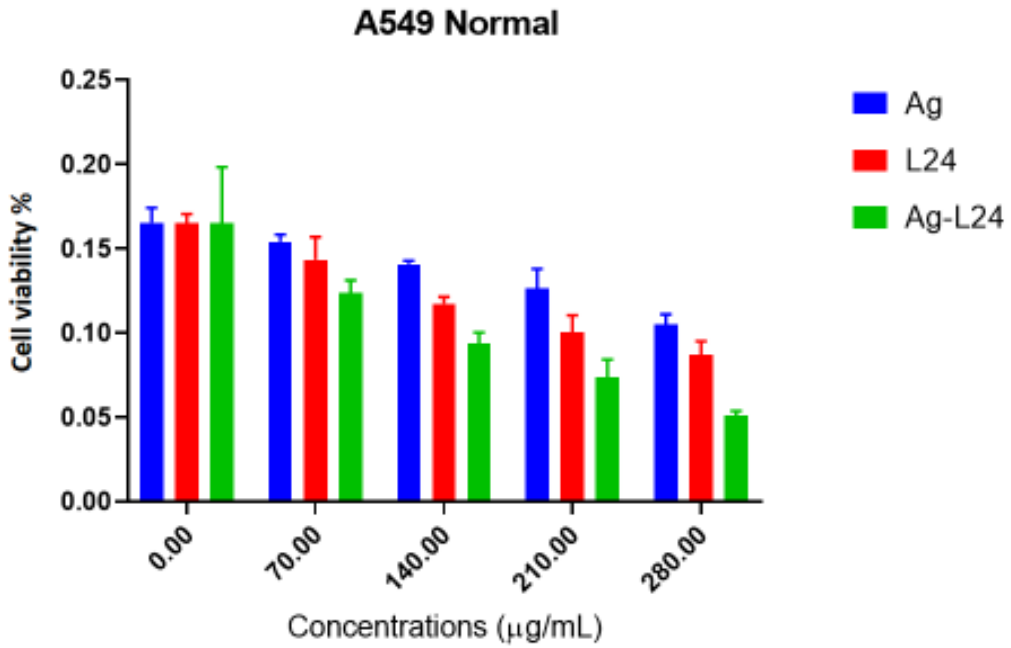

Figure 4.5. Graph representing 26% cell viability of A549 cell line versus logarithm of the concentration and IC50 values. Graph representing cell viability percentage of A549 cell line versus logarithm of the concentration of 70 and IC50 values. The cell viability % obtained at 70ug/ml for L24 was 70%, 79% of Ag and 57% cell viability for Ag-L24 after the incubation (without using laser). As the concentration increased the IC value of cell viability decreased. Ag-L24 shows maximum cell inhibitory growth as compared to Ag & L24 alone as shown in the graph.

4.2.1. MTT Assay results for A-549 cancer cell line After Laser

By using the MTT assay on malignant A-549 cell lines, the effect of the combination of the Ag-L24, L24, and the AgNps on cell viability was evaluated. The tests were carried out in triplicate and each cancerous cell line A549 was exposed to laser (A549-l) for 30 seconds. The main purpose of the laser was to increase the temperature of cells to cause hyperthermia to analyzed the effects of each treatment on cultured cell line . The concentrations of L24, Nps, and Ag-L24 were steadily increased from 0 to 3ug/mL. As seen in the graph (figure 4.6), combination treatment (green bar) shown reduced cell viability compared to single

drug treatment (red and blue bar). The IC value for each AgNPs, L24 and Ag-L24 coupling was calculated seprately (table 4.3). IC value displayed in the table 4 was determined by taking the log: conc. The IC50 value quantifies the amount of an inhibitory drug, substance, extract, or fraction required to inhibit a biological component by 50%. The IC value after the laser exposure of A549 cell line was calculated for L24 was 13, Ag 85.7 and Ag-L24 was 2.29.

Table 4.3. IC value calculated from IC50 for each treatment for A549-Laser.

Number	Name	IC Value for A549-L
1	L24	30.06
2	Ag	85.79
3	Ag-L24	2.29

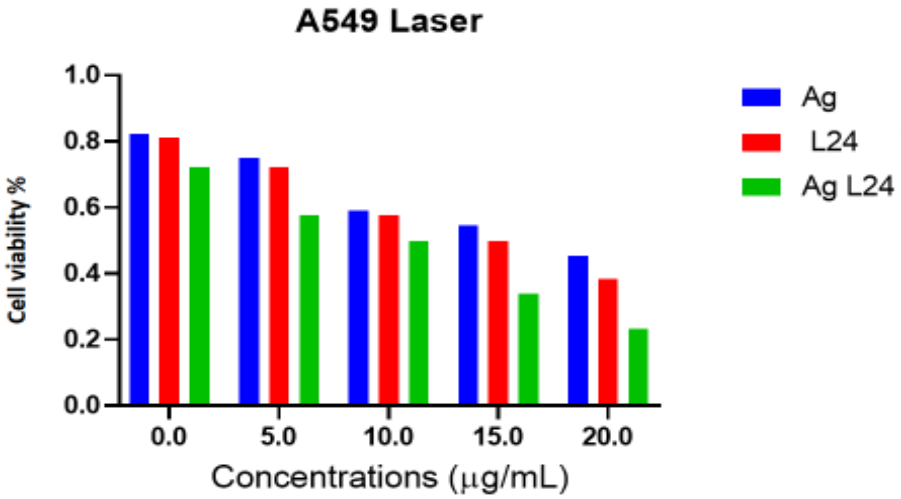

Figure 4.6. Graph representing cell viability percentage of A549 cell line versus logarithm of the concentration of 5, 10,15, 20 ug/mL and calculated from IC50 values.The cell viability % obtained at 5.0ug/ml for L24 was 65%, 69% of Ag at and 56% cell viability for Ag-L24 after the exposure of laser during incubation. As the concentration increased the IC value of cell viability decreased. Ag-L24 shows maximum cell inhibitory growth as compared to Ag & L24 alone as shown in the graph.

4.2.2. MTT Assay results of Beas2B cell line normal (without Laser)

The MTT test was used to determine cell viability %. The data are shown as a percentage of control cells' viability rate. Table 4.4 has a representation of IC values for each treatment. By using the MTT assay on Normal Beas2B cell lines, the effect of the combination of the Ag-L24, L24, and the AgNps on cell viability was evaluated. There was no laser utilized to increase the temperature of the cells during the triplicate studies. The concentrations of L24, Nps, and Ag-L24 were gradually increased from 0 to 3ug/mL times the IC50. According to the graph figure 4.6, combination treatment (Ag-L24,green bar) had a lower rate of cell viability % than single medication treatment (red and blue bar).). IC value displayed in the table 4.4 was determined by taking the log: conc. The IC50 value quantifies the amount of an inhibitory drug, substance, extract, or fraction required to inhibit a biological component by 50%. The IC value was calculated for L24 was 110.8, Ag 27.25 and Ag-L24 was 11.47.

Table 4.4. IC value calculated from IC50 for each treatment for BEAS2B normal.

Number	Name	IC Value for BEAS2B-N
1	L24	110.8
2	Ag	27.25
3	Ag-L24	11.47

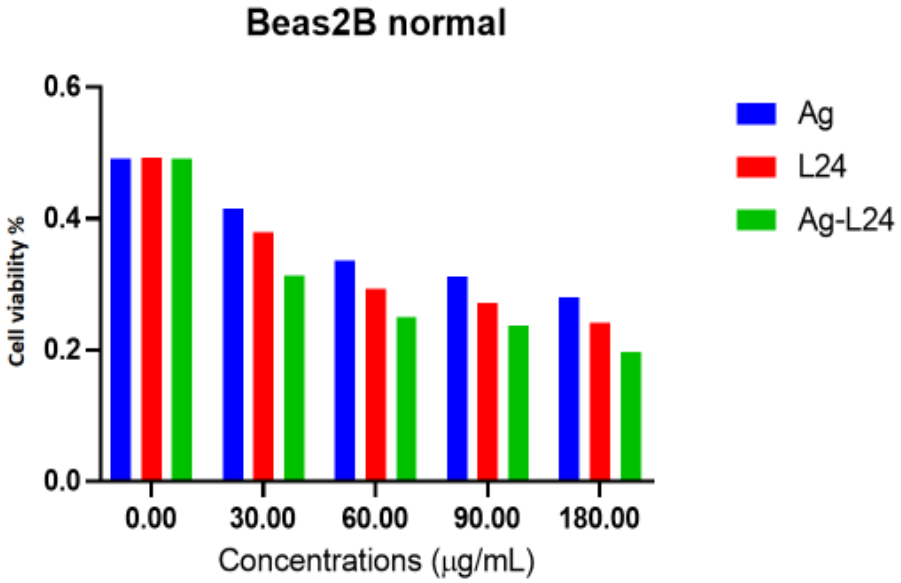

Figure 4.7. Graph representing cell viability percentage of Beas2B cell line versus logarithm of the concentration of 60 and IC50 values. The cell viability % obtained at 60ug/ml for L24 was 70%, 79% of Ag at and 57% cell viability for Ag-L24 after the incubation (without using laser). As the concentration increased the IC value of cell viability decreased. The results are expressed as the percentage of the viability rate of normal healthy Beas2B cells. All values are represented as the normal cells are not that much damaged at minimum concentration.

4.2.3. MTT Assay results for BEAS2B cell line After Laser

By using the MTT assay on Normal Beas2B cell lines, the effect of the combination of the Ag-L24, L24, and the AgNps on cell viability was evaluated. Cell line BEAS2B was exposed to laser for 30 seconds. The main purpose of the laser was to increase the temperature of cells to cause hyperthermia to analyzed the effects of each treatment on cultured cell line . The concentrations of L24, Nps, and Ag-L24 were steadily increased from 0 to 3ug/mL. As seen in the graph (figure 4.8), combination treatment (green bar) shown reduced cell viability compared to single drug treatment (red and blue bar). The IC value for each AgNPs, L24 and Ag-L24 coupling was calculated seprately (table 6). IC value displayed in the table 6 was determined by taking the log: conc. The IC50 value quantifies the amount of

an inhibitory drug, substance, extract, or fraction required to inhibit a biological component by 50%. The IC value after the laser exposure of BEAS2B cell line was calculated for L24 was 25.37, Ag 92.90 and Ag-L24 was 5.843.

Table 4.5. IC value calculated from IC50 for each treatment for BEAS2B normal.

Number	Name	IC Value for BEAS2B-L
1	L24	25.37
2	Ag	92.90
3	Ag-L24	5.843

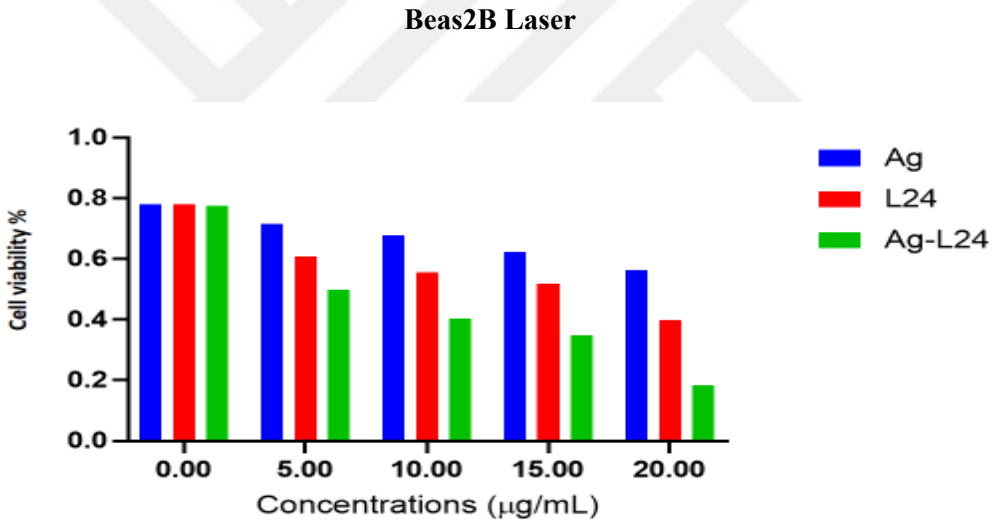

Figure 4.8. Graph representing cell viability percentage of Beas2B cell line versus logarithm of the concentration of 10 and IC50 values. The cell viability % obtained at 10ug/ml for L24 was 72%, 79% of Ag at and 58% cell viability for Ag-L24 after the exposure of laser during incubation. As the concentration increased the IC value of cell viability decreased. The results are expressed as the percentage of the viability rate of normal healthy Beas2B cells.

4.3. Discussion:

Silver nanoparticles can be an innovative approach for cancer treatment, in two perspectives: they reveal intrinsic anticancer properties, and can be used as carriers of anticancer drugs, enabling a therapeutic of dual treatment (Sofi, M *et al*., 2021). Silver nanoparticles have been increasingly investigated due to their peculiar physical, chemical, and optical properties, which allows them to cover several applications, namely in the transport of drugs to a specific target in the body. Given the limitations of conventional cancer chemotherapy, which include low bioavailability and the consequent use of high doses that cause adverse effects, strategies that overcome these difficulties are extremely important. Silver nanoparticles can be very useful in the transport of anticancer drugs, overcoming some of the difficulties of conventional therapies. The strategy of coupling anticancer agents to silver nanoparticles seems to have emerged promising therapeutic in the last decade (Helena Gomes., *et al*., 2021).

AgNPs coupled with pharmaceutical anticancer drugs were selected for this study. silver nano particles was combined and encapsulate with the chemotherapeutic drug (L24) and the efficacy of this system in the cancer cell line A549 & Beas2B in vitro conditions was assessed. The single treatment of each Ag & L24 was also given to the A549 & Beas2B cell lines to check the results. Straight 570nm laser was also used to expose the both cell lines to analyzed the effect of each treatment due to hyperthermia produced by laser for 30 seconds (Elsayed, K. *et al*, .2022). The cellular viability method used and the obtained results, expressed as a percentage of cell viability or as IC_{50} (concentration of the nanocarrier that causes the death of 50% of the cells, in this case) Dubbelboer, *et al* 2019).

After the assembly of AgNPs-L24, the anticancer activity of the free drug L24, AgNPs, and AgNPs-L24, was evaluated against lung carcinoma cell line (A-549) (Muhamad, M., *et al*., 2022). The free drug L24 originated IC_{50} values are 47.66 (normal), 30.06 (laser), after the incubation of 48h with the concentration of

280ug/mL for normal and 20 µg/mL for laser, respectively; the AgNPs originated IC_{50} values of 81.11(normal), 85.79 (laser) after the incubation of 48h with the concentration of 280ug/mL for normal and 20 µg/mL for laser ; while AgNPs-L24 allowed to obtain lower values: 6(normal), 2.29 (laser), after the incubation of 48h with the concentration of 280ug/mL for normal and 20 µg/mL for laser . It was evident the synergistic effect between AgNPs and L24 drug (AgNPs-L24) on the A549 cell line (IC_{50} = 30 µg/mL for free L24, IC_{50} = 85 µg/mL for AgNPs and IC_{50} = 2 µg/mL for AgNPs-L24, at 48 h). This means that for the same anticancer effect, a lower dose of AgNPs-L24 was required compared to free L24 (Yuan, Y. *et al*., 2018).

Same 570nm straight Laser exposure was given to the normal cell line Beas2B after the application of treatments Ag, L24 & Ag-L24. MTT assay results IC50 value calculated. For L24 drug the IC_{50} values are 110 (normal), 25.06 (laser), after the incubation of 48h with the concentration of 180ug/mL for normal and 20 µg/mL for laser respectively; the AgNPs originated IC_{50} values of 27.11(normal), 92 (laser) after the incubation of 48h with the concentration of 180ug/mL for normal and 20 µg/mL for laser ; while AgNPs-L24 allowed to obtain lower values: 11(normal), 5.89 (laser), after the incubation of 48h with the concentration of 180ug/mL for normal and 20 µg/mL for laser respectively.

The Combination of L24 drug and AgNps was highly synergistic in carcinoma of the lung A549 cell line, in vitro MTT Assay. It was observed that the minimum dosage of Ag-L24 cause more damage to the A549 cell line as compare to the drug L24 used alone. Ag-L24 with laser exposure show lowest IC value and cause more damage to A549 cancer cell line as compared to normal Beas2B healthy cell. It was also observed that the exposure of laser causing hyperthermia to release/activate the Ag-L24 in the cell in-between incubation period. Because hyperthermia increases temperature, AgNPs burst, drug release and cause damage to cells Cancerous cells structure also disrupt because of increasing temperature (Dong, F *et al*., 2016). The results obtained from the exposure of the laser was

much promising than that of Normal because the results with laser has lower IC-50 value.It was clearly observed that the coupling effect of Ag-L24 was very promising as compare to the other single treatments (Ag & L24). The IC value calculated after laser exposure in both cell lines A549 (IC50; 2) & Beas2B (IC50; 5.8) was very low as compared to other treatments. Meanwhile if compare these both IC50 values the lowest IC50 value was calculated for A549 cell line was 2 which is the lowest IC value for this A549-L treated with Ag-L24 coupling as compared to the normal cell line Beas2B.

The limitation for this study is that this coupling is causing nearly the same cytotoxic damage to normal and cancerous cell line with 10% difference as discussed above. As the coupling of Ag-L24 cause more cytotoxic damage to the cell so this coupling of Ag nano-particles and l24 drug is also a cytotoxic for normal cells. This combination is causing cell death not only in cancerous but in normal cells too. So there is a need to add specific receptors and ligands at the surface of silver nanoparticles so that they attach just with specific cells, that deliver the drug directly to the targeted tissue or cell without leaking drug in the blood or body. The drug delivery system will insure the covering and safety of the other cell from the drug. This resultant outcome limits the direct use of this coupling of drug in a living system.

But the strength of this study is that the coupling of Ag-L24 caused much damage to cancerous cells as compared to drug or silver alone. IC50 value of drug with encapsulation is very low that proves that low amount of drug needed to kill cancerous cells as compared to drug alone. Also with minimum low concentration 20ug/mL cause more damage to A549-L (when exposed to the 570nm straight laser) cell line as compared to Beas2B-L. That proves that when we use laser, because of hyperthermia much damage occur in cancerous cells as compared to normal cells because hyerthermia affects cancerous cell more as compared to normal cells. Normal cells survive with increasing temperature while cancerous cell donot survive, their structure disrupt, and drug enter very easily as compare to

normal cells.. So, this drug delivery system has a strength to kill maximum cancerous cells in encapsulation form (AgNPs-L24) as compared to drug alone. IC-50 value of drug used in encapsulation is much low as compared to drug alone. This result is very promising for the future use and manipulation of the drugs with minimum dose response.

5. CONCLUSION

The research study was conducted with the aim of reducing side effect of chemotherapy, radiotherapy against cancer. The drugs we are using are not only damaging cancer cells but normal cells also and bioavailability is also a problem. So, according to above data that shows in results section (table & graphs), the best results were shown when drug and Nps (AG-L24) were used in combined form. It was not only effective but it also increases the bioavailability of cancer drug when exposed to the laser. So if drug is used alone, then it needs in much amount of to reach our target because it also absorb into normal cells and damage them. On the other hand, if drug is used with cover of silver nanoparticle it is not only less toxic to our normal body cells but also use in very less quantity.

REFERENCES

Akbarzadeh A, Samiei M, Davaran S: Magnetic nanoparticles: preparation, physical properties, and applications in biomedicine. Nanoscale Res Lett 2012, 7:144.

Akbarzadeh A, Samiei M, Joo SW, Anzaby M, Hanifehpour Y, Nasrabadi HT, Davaran S: Synthesis, characterization and in vitro studies of doxorubicinloaded magnetic nanoparticles grafted to smart copolymers on A549 lung cancer cell line. J Nanobiotechnology 2012, 10:46.

Akbarzadeh, A., Rezaei-Sadabady, R., *et al.* (2013). Liposome: classification, preparation, and applications. *Nanoscale Research Letters* *8*(1). DOI: 10.1186/1556-276X-8-102.

Amarnath S, Sharma US: Liposomes in drug delivery: progress and limitations. Int J Pharm 1997, 154:123–140.

Andreas W, Karola VU: Liposome technology for industrial purposes. J Drug Deliv 2011, 2011:9.

Atrooz OM: Effects of alkylresorcinolic lipids obtained from acetonic extract of Jordanian wheat grains on liposome properties. Int J Biol Chem 2011, 5(5):314–321.

Bally M., K. Bailey, K. Sugihara, D. Grieshaber, J. Vor ¨ os, ¨ B. St¨ aler, Liposome and lipid bilayer arrays towards biosensing applications, Small (2010), https://doi.org/ 10.1002/smll.201000644.

Banerjee R, Tyagi P, Li S, Huang L: Anisamide-targeted stealth liposomes: a potent carrier for targeting doxorubicin to human prostate cancer cells. Int J Cancer 2004, 112:693–700.

Baselga J, Metselaar JM: Monoclonal antibodies: clinical applications: monoclonal antibodies directed against growth factor receptors. In Principles and Practice of Biological Therapy of Cancer. Edited by Rosenburg SA. Philadelphia: Lippincott; 2000:475–489.

Batzri S, Korn ED: Single bilayer liposomes prepared without sonication. Biochim Biophy Acta 1973, 298(4):1015–1019.

Deamer D, Bangham AD: Large volume liposomes by an ether vaporization method. Biochim Biophys Acta 1976, 443(3):629–634.

Du, W., & Elemento, O. (2015). Cancer systems biology: embracing complexity to develop better anticancer therapeutic strategies. *Oncogene*, *34*(25), 3215-3225.

Eid K.A.M., H.M.E. Azzazy, Sustained broad-spectrum antibacterial effects of nanoliposomes loaded with silver nanoparticles, Nanomedicine. (2014), https:// doi.org/10.2217/nnm.13.89.

Espinoza, J. T., Novak, R. S., Magalhães, C. G., Budel, J. M., Justus, B., Gonçalves, M. M., ... & Paula, J. D. F. P. D. (2021). Preparation and characterization of liposomes loaded with silver nanoparticles obtained by green synthesis. *Brazilian Journal of Pharmaceutical Sciences*, *56*.

Frolov VA, Shnyrova AV, Zimmerberg J. Lipid polymorphisms and membrane shape. Cold Spring Harb Perspect Biol. 2011;3:a004747.

Gabizon A: Liposomes as a drug delivery system in cancer therapy. In Drug Carrier Systems. Edited by Roerdink FHD, Kron AM. Chichester: Wiley; 1989:185–211.

Gala, U. H., Miller, D. A., & Williams III, R. O. (2020). Harnessing the therapeutic potential of anticancer drugs through amorphous solid dispersions. *Biochimica et Biophysica Acta (BBA)-Reviews on Cancer*, *1873*(1), 188319.

Gala, U. H., Miller, D. A., & Williams III, R. O. (2020). Harnessing the therapeutic potential of anticancer drugs through amorphous solid dispersions. *Biochimica et Biophysica Acta (BBA)-Reviews on Cancer*, *1873*(1), 188319.

Ge G., H. Wu, F. Xiong, Y. Zhang, Z. Guo, Z. Bian, J. Xu, C. Gu, N. Gu, X. Chen, D. Yang, The cytotoxicity evaluation of magnetic iron oxide nanoparticles on human aortic endothelial cells, Nanoscale Res. Lett. (2013), https://doi.org/ 10.1186/1556-276X-8-215.

Govindaraju K., K. Krishnamoorthy, S.A. Alsagaby, G. Singaravelu, M. Premanathan, Green synthesis of silver nanoparticles for selective toxicity towards cancer cells, IET Nanobiotechnol. (2015), https://doi.org/10.1049/ietnbt.2015.0001.

Hemanthkumar M, Spandana V: Liposomal encapsulation technology a novel drug delivery system designed for ayurvedic drug preparation. IRJP 2011, 2(10):4–7.

Himanshu A, Sitasharan P, Singhai AK: Liposomes as drug carriers. IJPLS 2011, 2(7):945–951.

Ivanova N., V. Gugleva, M. Dobreva, I. Pehlivanov, S. Stefanov, V. Andonova, Silver nanoparticles as multi-functional drug delivery systems, Nanomedicines, IntechOpen, 2019, https://doi.org/10.5772/intechopen.80238.

Jia, H. R., Zhu, Y. X., Duan, Q. Y., Chen, Z., & Wu, F. G. (2019). Nanomaterials meet zebrafish: Toxicity evaluation and drug delivery applications. *Journal of Controlled Release*, *311*, 301-318.

Kalashnikova I., S. Das, S. Seal, Nanomaterials for wound healing: Scope and advancement, Nanomedicine. (2015), https://doi.org/10.2217/nnm.15.82.

Kaphle, A., Nagaraju, N., & Daima, H. K. (2018). Contemporary developments in nanobiotechnology: applications, toxicity, sustainability, and future perspective. In *Nanobiotechnology* (pp. 1-34). CRC Press.

Kataria S, Sandhu P, Bilandi A, Akanksha M, Kapoor B, Seth GL, Bihani SD: Stealth liposomes: a review. IJRAP 2011, 2(5):1534–1538.

Khorrami, S., Zarrabi, A., Khaleghi, M., Danaei, M., & Mozafari, M. R. (2018). Selective cytotoxicity of green synthesized silver nanoparticles against the MCF-7 tumor cell line and their enhanced antioxidant and antimicrobial properties. *International journal of nanomedicine*, *13*, 8013.

Kim S., D.Y. Ryu, Silver nanoparticle-induced oxidative stress, genotoxicity and apoptosis in cultured cells and animal tissues, J. Appl. Toxicol. (2013), https://doi. org/10.1002/jat.2792.

Kovacs D., ´ N. Igaz, C. Keskeny, P. B´elteky, T. Toth, ´ R. G´ aspar, ´ D. Madarasz, ´ Z. R´ azga, Z. Konya, ´ I.M. Boros, M. Kiricsi, Silver nanoparticles defeat p53-positive and p53-negative osteosarcoma cells by triggering mitochondrial stress and apoptosis, Sci. Rep. 6 (2016) 27902, https://doi.org/10.1038/srep27902.

Kunisawa J, Mayumi T: Fusogenic liposome delivers encapsulated nanoparticles for cytosolic controlled gene release. J Control Release 2005, 105:344–353.

Liu L, Yonetaini T: Preparation and characterization of liposomeencapsulated haemoglobin by a freeze-thaw method. J Microencapsulation 1994, 11(4):409–421.

Liu, E., Zhang, M., Cui, H., Gong, J., Huang, Y., Wang, J., ... & Yang, V. C. (2018). Tat-functionalized Ag-Fe3O4 nano-composites as tissue-penetrating vehicles for tumor magnetic targeting and drug delivery. *Acta pharmaceutica sinica B*, *8*(6), 956-968.

Lopes V.R., Loitto V., Audinot J.N., Bayat N., A.C. Gutleb, S. Cristobal, Dosedependent autophagic effect of titanium dioxide nanoparticles in human HaCaT cells at non-cytotoxic levels, J. Nanobiotechnology. (2016), https://doi.org/ 10.1186/s12951-016-0174-0.

Mao B.H., J.C. Tsai, C.W. Chen, S.J. Yan, Y.J. Wang, Mechanisms of silver nanoparticle-induced toxicity and important role of autophagy, Nanotoxicology. (2016), https://doi.org/10.1080/17435390.2016.1189614.

Maria Laura I, Franco D, Cattel L: Stealth liposomes: review of the basic science, rationale, and clinical applications, existing and potential. Int J Nanomedicine 2006, 1(3):297–315.

Mayer LD, Bally MB, Hope MJ, Cullis PR: Techniques for encapsulating bioactive agents in to liposomes. Chem Phys Lipids 1986, 40:333–345.

McShan D., P.C. Ray, H. Yu, Molecular toxicity mechanism of nanosilver, J. Food Drug Anal. (2014), https://doi.org/10.1016/j.jfda.2014.01.010.

Mehta K, Sadeghi T, McQueen T, Lopez-Berestein G: Liposome encapsulation circumvents the hepatic clearance mechanisms of alltrans-retinoic acid. Leuk Res 1994, 18:587–596.

Miyayama T., M. Matsuoka, Involvement of lysosomal dysfunction in silver nanoparticle-induced cellular damage in A549 human lung alveolar epithelial cells, J. Occup. Med. Toxicol. (2016), https://doi.org/10.1186/s12995-016-0090-0.

Mohammed Fayaz A, K. Balaji, M. Girilal, P.T. Kalaichelvan, R. Venkatesan, Mycobased synthesis of silver nanoparticles and their incorporation into sodium alginate films for vegetable and fruit preservation, J. Agric. Food Chem. (2009), https://doi.org/10.1021/jf900337h.

Navya, P. N., & Daima, H. K. (2016). Rational engineering of physicochemical properties of nanomaterials for biomedical applications with nanotoxicological perspectives. *Nano Convergence*, *3*(1), 1-14.

Niska K., E. Zielinska, M.W. Radomski, I. Inkielewicz-Stepniak, Metal nanoparticles in dermatology and cosmetology: Interactions with human skin cells, Chem. Biol. Interact. (2018), https://doi.org/10.1016/j.cbi.2017.06.018.

Othman, A. K., El Kurdi, R., Badran, A., Mesmar, J., Baydoun, E., & Patra, D. (2022). Liposome-based nanocapsules for the controlled release of dietary curcumin: PDDA and silica nanoparticle-coated DMPC liposomes enhance the fluorescence efficiency and anticancer activity of curcumin. *RSC advances*, *12*(18), 11282-11292.

Papahadjopoulos D, Kimelberg HK. *Progress in Surface Science*. Oxford: Pergamon; 1973. Phospholipid vesicles (liposomes) as models for biological membranes: their properties and interactions with cholesterol and proteins; pp. 141–149.

Parthasarathy R, Sacks PC, Harris D, Brock H, Mehta K: Interaction of liposorae-associated all-trans-retinoic acid with squamous carcinoma cells. Cancer Chemother Pharmacol 1994, 34:527–534.

Pick U: Liposomes with a large trapping capacity prepared by freezing and thawing of sonicated phospholipid mixtures. Arch Biochem Biophys 1981, 212:186–194.

Prasanna, A., Pooja, R., Suchithra, V., Ravikumar, A., Gupta, P. K., & Niranjan, V. (2018). Smart drug delivery systems for cancer treatment using nanomaterials. *Materials Today: Proceedings*, *5*(10), 21047-21054.

Rasoulzadehzali, M., & Namazi, H. (2018). Facile preparation of antibacterial chitosan/graphene oxide-Ag bio-nanocomposite hydrogel beads for controlled release of doxorubicin. *International journal of biological macromolecules*, *116*, 54-63.

Reidy B, A. Haase, A. Luch, K. Dawson, I. Lynch, Mechanisms of Silver Nanoparticle Release, Transformation and Toxicity: A Critical Review of Current Knowledge and Recommendations for Future Studies and Applications, Materials (Basel). 6 (2013), https://doi.org/10.3390/ma6062295.

Riaz M: Liposome preparation method. Pak J Pharm Sci 1996, 9(1):65–77.

Romberg B, Hennink WE, Storm G: Sheddable coatings for long-circulating nanoparticles. Pharm Res 2008, 25(1):55–71.

Saesoo, S., Bunthot, S., Sajomsang, W., Gonil, P., Phunpee, S., Songkhum, P., & Saengkrit, N. (2016). Phospholipid-chitosan hybrid nanoliposomes promoting cell entry for drug delivery against cervical cancer. *Journal of colloid and interface science*, *480*, 240-248.

Sanpui P., A. Chattopadhyay, S.S. Ghosh, Induction of apoptosis in cancer cells at low silver nanoparticle concentrations using chitosan nanocarrier, ACS Appl. Mater. Interfaces (2011), https://doi.org/10.1021/am100840c.

Sercombe, L., Veerati, T., Moheimani, F., Wu, S. Y., Sood, A. K., & Hua, S. (2015). Advances and challenges of liposome assisted drug delivery. *Frontiers in pharmacology*, *6*, 286.

Shaheen SM, Shakil Ahmed FR, Hossen MN, Ahmed M, Amran MS, Ul-Islam MA: Liposome as a carrier for advanced drug delivery. Pak J Biol Sci 2006, 9(6):1181–1191.

Shrestha ,B., L. Tang, G. Romero, Nanoparticles-mediated combination therapies for cancer treatment, Adv. Ther. 2 (2019) 1900076, , https://doi.org/10.1002/adtp. 201900076.

Sofi, M. A., Sunitha, S., Sofi, M. A., Pasha, S. K., & Choi, D. (2021). An overview of antimicrobial and anticancer potential of silver nanoparticles. *Journal of King Saud University-Science*, 101791.

Son, G. H., Lee, B. J., & Cho, C. W. (2017). Mechanisms of drug release from advanced drug formulations such as polymeric-based drug-delivery systems and lipid nanoparticles. *Journal of Pharmaceutical Investigation*, *47*(4), 287-296.

Song H, Geng HQ, Ruan J, Wang K, Bao CC, Wang J, Peng X, Zhang XQ, Cui DX: Development of polysorbate 80/phospholipid mixed micellar formation for docetaxel and assessment of its in vivo distribution in animal models. Nanoscale Res Lett 2011, 6:354.

Soni, N., Jyoti, K., Jain, U. K., Katyal, A., Chandra, R., & Madan, J. (2017). Noscapinoids bearing silver nanocrystals augmented drug delivery, cytotoxicity, apoptosis and cellular uptake in B16F1, mouse melanoma skin cancer cells. *Biomedicine & pharmacotherapy*, *90*, 906-913.

Sreekanth, T. V. M., Nagajyothi, P. C., Muthuraman, P., Enkhtaivan, G., Vattikuti, S. V. P., Tettey, C. O., & Yoo, K. (2018). Ultra-sonication-assisted silver nanoparticles using Panax ginseng root extract and their anti-cancer and antiviral activities. *Journal of Photochemistry and Photobiology B: Biology*, *188*, 6-11.

Stensberg M.C., Q. Wei, E.S. McLamore, D.M. Porterfield, A. Wei, M.S. Sepúlveda, Toxicological studies on silver nanoparticles: Challenges and opportunities in assessment, monitoring and imaging, Nanomedicine. (2011), https://doi.org/ 10.2217/nnm.11.78.

Storm G, Roerdink FH, Steerenberg PA, de Jong WH, Crommelin DJA: Influence of lipid composition on the antitumor activity exerted by doxorubicin containing liposomes in a rat solid tumor model. Cancer Res 1987, 47:3366–3372.

Sun, Q., Gao, H., Sukhorukov, G. B., & Routh, A. F. (2017). Silver-coated colloidosomes as carriers for an anticancer drug. *ACS applied materials & interfaces*, *9*(38), 32599-32606.

Szoka F Jr, Papahadjopoulos D: Procedure for preparation of liposomes with large internal aqueous space and high capture by reverse-phase evaporation. Proc Natl Acad Sci USA 1978, 75(9):4194–4198.

Tao, J., Ding, W. F., Che, X. H., Chen, Y. C., Chen, F., Chen, X. D., ... & Xiong, S. B. (2016). Optimization of a cationic liposome-based gene delivery system for the application of miR-145 in anticancer therapeutics. *International journal of molecular medicine*, *37*(5), 1345-1354.

Thompson E.A., E. Graham, C.M. Macneill, M. Young, G. Donati, E.M. Wailes, B. T. Jones, N.H. Levi-Polyachenko, Differential response of MCF7, MDA-MB-231, and MCF 10A cells to hyperthermia, silver nanoparticles and silver nanoparticleinduced photothermal therapy, Int. J. Hyperth. (2014), https://doi.org/10.3109/ 02656736.2014.936051.

Wagner A, M. Platzgummer, G. Kreismayr, H. Quendler, G. Stiegler, B. Ferko, G. Vecera, K. Vorauer-Uhl, H. Katinger, GMP production of liposomes–a new industrial approach, J. Liposome Res. 16 (2006) 311–319, https://doi.org/ 10.1080/08982100600851086.

Wang, X., Zhang, H., & Chen, X. (2019). Drug resistance and combating drug resistance in cancer. *Cancer Drug Resistance*, *2*(2), 141.

Yusuf A, A. Casey, Evaluation of silver nanoparticle encapsulation in DPPC-based liposome by different methods for enhanced cytotoxicity, Int. J. Polym. Mater. Polym. Biomater. (2019), https://doi.org/10.1080/00914037.2019.1626390.

Yusuf, A., Brophy, A., Gorey, B., & Casey, A. (2018). Liposomal encapsulation of silver nanoparticles enhances cytotoxicity and causes induction of reactive oxygen species-independent apoptosis. *Journal of Applied Toxicology*, *38*(5), 616-627.

Zanette C., M. Pelin, M. Crosera, G. Adami, M. Bovenzi, F.F. Larese, C. Florio, Silver nanoparticles exert a long-lasting antiproliferative effect on human keratinocyte HaCaT cell line, Toxicol Vitr. 25 (2011) 1053–1060, https://doi.org/10.1016/j. tiv.2011.04.005.

CURRICULUM VITAE

Syed Hamza Zaffar BUKHARİ, received his Bachelor degree in biotechnology from International Islamic University Islamabad. He worked as an internee in National Institute of health Islamabad during his bachelor degree. He joined Çukorova University Adana Turkey for his Masters degree and worked under the supervision of Dr. Yasemin saygıdeğer in Saygıdeğer lab..His perspective research areas are Molecular biotechnology, Nanotechnology and Genetic engineering. His aim is to improve and contribute towards healthy life and enhance the quality of life in society through visualisation and analysis.